

**Memorandum Report
for
SERDP Project WP-2244**

“Scientific Basis for Paint Stripping: Elucidated Combinatorial Mechanism of Methylene Chloride and Phenol Based Paint Removers”

10 October 2013

Prepared by:

James H. Wynne, PhD and Grant C. Daniels

Chemistry Division

US Naval Research Laboratory

4555 Overlook Ave, SW Code 6124

Washington, DC 20375

Clive R. Clayton, PhD and Christopher N. Young

Department of Materials Science and Engineering

Stony Brook University

Stony Brook, NY 11794

Report Documentation Page			Form Approved OMB No. 0704-0188	
<p>Public reporting burden for the collection of information is estimated to average 1 hour per response, including the time for reviewing instructions, searching existing data sources, gathering and maintaining the data needed, and completing and reviewing the collection of information. Send comments regarding this burden estimate or any other aspect of this collection of information, including suggestions for reducing this burden, to Washington Headquarters Services, Directorate for Information Operations and Reports, 1215 Jefferson Davis Highway, Suite 1204, Arlington VA 22202-4302. Respondents should be aware that notwithstanding any other provision of law, no person shall be subject to a penalty for failing to comply with a collection of information if it does not display a currently valid OMB control number.</p>				
1. REPORT DATE 10 OCT 2013	2. REPORT TYPE	3. DATES COVERED 00-00-2013 to 00-00-2013		
4. TITLE AND SUBTITLE Scientific Basis for Paint Stripping: Elucidated Combinatorial Mechanism of Methylene Chloride and Phenol Based Paint Removers			5a. CONTRACT NUMBER	
			5b. GRANT NUMBER	
			5c. PROGRAM ELEMENT NUMBER	
6. AUTHOR(S)			5d. PROJECT NUMBER	
			5e. TASK NUMBER	
			5f. WORK UNIT NUMBER	
7. PERFORMING ORGANIZATION NAME(S) AND ADDRESS(ES) Naval Research Laboratory, Chemistry Division, 4555 Overlook Ave, SW Code 6124, Washington, DC, 20375			8. PERFORMING ORGANIZATION REPORT NUMBER	
9. SPONSORING/MONITORING AGENCY NAME(S) AND ADDRESS(ES)			10. SPONSOR/MONITOR'S ACRONYM(S)	
			11. SPONSOR/MONITOR'S REPORT NUMBER(S)	
12. DISTRIBUTION/AVAILABILITY STATEMENT Approved for public release; distribution unlimited				
13. SUPPLEMENTARY NOTES				
14. ABSTRACT				
15. SUBJECT TERMS				
16. SECURITY CLASSIFICATION OF:			17. LIMITATION OF ABSTRACT Same as Report (SAR)	18. NUMBER OF PAGES 46
a. REPORT unclassified	b. ABSTRACT unclassified	c. THIS PAGE unclassified		

TABLE OF CONTENTS

Acknowledgement	iv
Objective	1
Background	1
Previous Work.....	2
Materials and Methods.....	3
Chemicals	3
Coatings.....	3
Sample Exposure.....	5
Experimental Methods	6
Results and Discussion	7
Confocal and Scanning Electron Microscopy	7
Spectroscopy	10
Contact Angle and Surface Free Energy	26
Roughness Analysis	28
Thermal Analysis	31
Solution Ingress/Egress	37
Conclusion	39
Literature Cited	40
Meetings	40
References	41

LIST OF FIGURES

FIGURE 1: CONFOCAL FALSE COLOR THREE DIMENSIONAL IMAGES OF UNEXPOSED MIL-PRF-53039, LEFT, AND MIL-PRF-53039 EXPOSED TO METHYLENE CHLORIDE FOR SIXTY MINUTES, RIGHT	8
FIGURE 2: CONFOCAL FALSE COLOR THREE DIMENSIONAL AND COLOR IMAGE OF MIL-PRF-53039 EXPOSED TO METHYLENE CHLORIDE, ETHANOL, WATER, PHENOL FOR FORTY MINUTES	8
FIGURE 3: CONFOCAL IMAGES OF FILM DEPOSITION ON MIL-PRF-85825, LEFT SIDE, AND MIL-PRF-53039, RIGHT SIDE AFTER EXPOSURE TO METHYLENE CHLORIDE/ETHANOL/WATER.....	9
FIGURE 4: SEM IMAGES OF MIL-PRF-53039 EXPOSED TO METHYLENE CHLORIDE, ETHANOL, WATER AND METHOCEL	9
FIGURE 5: FTIR-ATR COMPARISON OF PARTIALLY FORMULATED MIL-PRF-53039	10
FIGURE 6: RAMAN SPECTRA OF METHOCEL AND MIL-PRF-53039 WITH FILM ON SURFACE	11
FIGURE 7: XPS SPECTRA OF MIL-PRF-53039.....	12
FIGURE 9: NEXAFS C K-EDGE SPECTRUM OF UNEXPOSED, FULLY-FORMULATED MIL-PRF-85285 (BLUE COLOR), BOTTOM SURFACE.....	15
FIGURE 10:NEXAFS C K-EDGE SPECTRUM OF UNEXPOSED, CLEAR-FORMULATED MIL-PRF-85285, TOP SURFACE ..	16
FIGURE 11: NEXAFS C K-EDGE SPECTRUM OF UNEXPOSED, CLEAR-FORMULATED MIL-PRF-85285, BOTTOM SURFACE.....	17
FIGURE 12: BLACK AND WHITE HYPERSPECTRAL IMAGE OF MC-EXPOSED, FULLY-FORMULATED MIL-PRF-85285, TOP SURFACE, WITH BRIGHTNESS LINKED TO C=C PI* PEAK AREA.	18
FIGURE 13: NEXAFS C K-EDGE SPECTRUM OF MC-EXPOSED, FULLY-FORMULATED MIL-PRF-85285, TOP SURFACE, WITHIN THE AREA OF THE METHYLENE CHLORIDE DROPLET.	18
FIGURE 14: NEXAFS C K-EDGE SPECTRUM OF MC-EXPOSED, FULLY-FORMULATED MIL-PRF-85285, TOP SURFACE, IN THE HALO-LIKE RING AROUND THE OUTER PERIMETER OF THE METHYLENE CHLORIDE DROPLET.	19
FIGURE 15: BLACK AND WHITE HYPERSPECTRAL IMAGE OF MC-EXPOSED, FULLY-FORMULATED MIL-PRF-85285, BOTTOM SURFACE, WITH BRIGHTNESS LINKED TO C=C PI* PEAK AREA.	20
FIGURE 16: NEXAFS C K-EDGE SPECTRUM OF MC-EXPOSED, FULLY-FORMULATED MIL-PRF-85285, BOTTOM SURFACE, WITHIN THE AREA OF THE METHYLENE CHLORIDE DROPLET.	20
FIGURE 17: NEXAFS C K-EDGE SPECTRUM OF MC-EXPOSED, FULLY-FORMULATED MIL-PRF-85285, BOTTOM SURFACE, IN THE HALO-LIKE RING AROUND THE OUTER PERIMETER OF THE METHYLENE CHLORIDE DROPLET.	21
FIGURE 18: BLACK AND WHITE HYPERSPECTRAL IMAGE OF PHOH/H ₂ O-EXPOSED, FULLY-FORMULATED MIL-PRF-85285, BOTTOM SURFACE (LEFT) AND TOP SURFACE (RIGHT), WITH BRIGHTNESS LINKED TO C=C PI* PEAK AREA.	22
FIGURE 19: NEXAFS C K-EDGE SPECTRUM OF PHOH/H ₂ O-EXPOSED, FULLY-FORMULATED MIL-PRF-85285, TOP SURFACE, IN THE REGION OF THE DROPLET.	22
FIGURE 20: NEXAFS C K-EDGE SPECTRUM OF PHOH/H ₂ O-EXPOSED, FULLY-FORMULATED MIL-PRF-85285, BOTTOM SURFACE, IN THE REGION OF THE DROPLET.	23
FIGURE 21: NEXAFS C K-EDGE SPECTRUM OF MC/EtOH/PHOH-EXPOSED, FULLY-FORMULATED MIL-PRF-85285, TOP SURFACE.	24
FIGURE 22: NEXAFS C K-EDGE SPECTRUM OF MC/EtOH/PHOH-EXPOSED, FULLY-FORMULATED MIL-PRF-85285, BOTTOM SURFACE.	24
FIGURE 23: CONTACT ANGLE AND SURFACE FREE ENERGY OF MIL-PRF-53039 EXPOSED TO PAINT STRIPPER SOLUTIONS.....	26
FIGURE 24: CONTACT ANGLE AND SURFACE FREE ENERGY OF MIL-PRF-85285 EXPOSED TO PAINT STRIPPER SOLUTIONS.....	27
FIGURE 25: TGA OVERLAY OF CLEAR MIL-PRF-53039 EXPOSED TO PAINT STRIPPER SOLUTIONS.....	31
FIGURE 26: TGA OVERLAY OF PARTIALLY FORMULATED MIL-PRF-53039 EXPOSED TO PAINT STRIPPER SOLUTIONS .	32
FIGURE 27: TGA OVERLAY OF MIL-PRF-53039 EXPOSED TO PAINT STRIPPER SOLUTIONS.....	33
FIGURE 28: TGA OVERLAY OF CLEAR MIL-PRF-85285 EXPOSED TO PAINT STRIPPER SOLUTIONS.....	34
FIGURE 29: TGA OVERLAY OF PARTIALLY FORMULATED MIL-PRF-85285 EXPOSED TO PAINT STRIPPER SOLUTIONS .	34

FIGURE 30: TGA OVERLAY OF MIL-PRF-85285 EXPOSED TO PAINT STRIPPER SOLUTIONS	35
FIGURE 31: METHYLENE CHLORIDE/ETHANOL/PHENOL WETTING MIL-PRF-85285	37

LIST OF TABLES

TABLE 1: COMPOSITION OF SOLVENT SOLUTIONS	3
TABLE 2: MIL-DTL-53039 SINGLE COMPONENT ALIPHATIC POLYURETHANE CARC	4
TABLE 3: MIL-PRF-85285 HIGH SOLIDS POLYURETHANE TOPCOAT	4
TABLE 4: MIL-DTL-53039 SINGLE COMPONENT ALIPHATIC POLYURETHANE CARC	4
TABLE 5: MIL-PRF-85285 HIGH SOLIDS POLYURETHANE TOPCOAT	5
TABLE 6: LABELS AND ASSIGNMENTS OF NEXAFS C K-EDGE PEAK FITS	14
TABLE 7: WATER CONTACT ANGLE AND SURFACE FREE ENERGY OF COATINGS	26
TABLE 8: ROUGHNESS OF MIL-PRF-53039	29
TABLE 9: ROUGHNESS OF MIL-PRF-85285	30
TABLE 10: GLASS TRANSITION TEMPERATURES OF EXPOSED COATINGS	36
TABLE 11: DYNAMIC CONTACT ANGLE AND COMPLETE WETTING TIME OF UNEXPOSED COATINGS	38
TABLE 12: DYNAMIC CONTACT ANGLE AND COMPLETE WETTING TIME OF EXPOSED COATINGS	38

List of Abbreviations

ATR – Attenuated Total Reflectance
CARC – Chemical Agent Resistant Coating
DSC – Differential Scanning Calorimetry
eV – electron Volt
FTIR – Fourier Transform Infrared
FWHM – Full Width Half Maximum
NEXAFS – Near Edge X-ray Adsorption Fine Structure
NMR – Nuclear Magnetic Resonance
SEM – Scanning Electron Microscope
SERDP - Strategic Environmental Research and Development Program
Tg – Glass Transition
TGA – Thermal Gravimetric Analysis
UV – Ultra Violet
VOC – Volatile Organic Compound
XPS – X-ray Photoelectron Spectroscopy

Acknowledgement

The development and formulation of the clear and partially formulated coating utilized in this work were made by Jack Kelley and his team at the Army Research Lab in Aberdeen Proving Ground. A short description of the work and list of components is included in this report.

Objective

The objective of this project is to elucidate the mechanism(s) of action of methylene chloride and phenol based paint strippers on polymeric coatings in order to lead to efficient, cost-effective, and safe alternatives. This is accomplished by monitoring the changes in physical and molecular-level properties of polymeric coatings after exposure to the components of organic solvent based paint strippers.

Background

Historically, chemical paint strippers based on methylene chloride and phenol were widely used to remove polymeric coatings. These strippers were highly effective, inexpensive and exhibited minimal impact on the substrate. However, environmental and health concerns suggest the need for replacements. Replacement attempts have led to more environmentally friendly alternatives at the cost of performance, price, and substrate damage [1]. The mechanism by which methylene chloride and phenol work to remove polymeric coatings has not been fully characterized, [2] despite over 50 years of research in this area [3]. One major avenue of investigation has been to analyze physical changes in relation to adhesion loss. The conclusion of this research has been that solvent-based paint removing solutions wet the paint surface and then penetrate the layers to the substrate by diffusion through the coating [4, 5]. It is thought that the small molar volume solvents, *i.e.* water and methylene chloride, are able to penetrate the coating by more easily “fitting” into spaces between the polymer molecules and diffusing through these spaces and channels[6]. Polarity and other physical properties of the solvent also play a strong role in the ability to solvate the coating. The physical changes to the coating, such as swelling, cause adhesion loss by disrupting the polymer layers and breaking hydrogen bonds or other intermolecular forces. Generally, swelling reduces the stress necessary to fracture the coating by increasing the strain on the polymer network. Experimentally this is seen by the ease of scraping off a solvated coating versus a dry coating from a substrate. There has been some investigation into the chemical interactions between solvents and the coating, [7] including evidence of the influence solvents have on the polymer structure.

To effectively elucidate the effect of chemical paint stripper on polymeric coatings, some well characterized control polymeric coatings are needed. Commercial coatings contain not only the binder but also various pigments, fillers, flattening compounds, pigment related dispersion and wetting agents. To reduce complications, some of this work employed control coatings made without these components.

The clear films were made of two military specified coatings including two polyurethane topcoats (MIL-SPEC: 53039 and 85285). Films of the same military specified coatings in their full formulation were also studied. As a final control limited studies were performed on partial

formulations of the specified coatings, that is, formulations containing all of the full formulation components except the flattening agents.

This work aims to use wet organic chemistry, thermal analysis, visible microscopy and spectroscopy and vibrational spectroscopy to understand the mechanism of how methylene chloride based paint removers remove polymeric coatings and so fill the knowledge gap in this area.

Previous Work

We reported the determination of the mode of action of methylene chloride and phenol in organic solvent based paint strippers. Clear versions and partial formulations of currently in use military coatings were created. The changes in physical and molecular-level properties of these clear coatings as well as the commercial equivalents after exposure to components of the paint stripper including methylene chloride and phenol were reported. The coatings were characterized using DSC, TGA, FTIR-ATR, Raman, XPS, and ^1H and ^2H solid-state NMR. Our results indicate that methylene chloride acts as a facilitator for the other solvents in penetrating the coating but methylene chloride itself is not responsible for coating degradation. ^1H NMR results show that methylene chloride solvates the coating and is in close contact with the polymer chains. Raman spectroscopy further confirms that methylene chloride solvates the carbonyl bond to cause dilation. Deuterium NMR confirms this by showing restriction to the tumbling of methylene chloride, likely due to some dipole-dipole interaction with the polymer as the solvent's interaction energy is relatively weak. DSC shows significant depression of the glass transition temperature of all the coatings after exposure to solvent mixtures containing phenol, but little change after exposure to methylene chloride. The control mixture containing multiple solvents from the paint stripper caused the greatest coating degradation, suggesting that while phenol is the principal agent in glass transition depression, the other solvents, particularly water, play a significant role.

FTIR-ATR and XPS results indicate a hydrolysis reaction occurring, at least at the surface, of samples exposed to methylene chloride/ethanol/water solutions. Nucleophilic attack of the polymer backbone by phenol is suggested by the thermal, vibrational and deuterium NMR spectroscopic data, although unambiguous confirmation of this reaction is still needed. Findings from vibrational spectroscopy have indicated a significant change in the chemical structures as a result of solvent exposure. This change is particular to the solvent mixture used, especially phenol exposure, which causes the greatest difference in the spectra. Solid-state ^1H NMR data suggest that the stripper components rapidly exert very significant effects that increase the polymer segmental dynamics in a fashion similar to what takes place in the untreated coatings by heating to much higher temperatures. Deuterium NMR of *d*2-MC (CD_2Cl_2) at various temperatures shows that the methylene chloride molecule present in a polyurethane topcoat is not rigid but rather undergoes isotropic rotational tumbling. The rate of tumbling however is orders of magnitude slower than that in solvents, suggestive of weak interactions with groups on the polymer, perhaps via electric dipoles. The deuterium NMR of an epoxy primer exposed to *d*5-phenol/ethanol for different lengths of time reveals a wealth of detailed dynamical information for each sample exposure from changes in the spectral appearance and the T2 as a function of temperature. Molecular dynamics behavior ranging from rigid phenyl rings on the phenol, to 180° ring flips, to anisotropic motions of varying amplitudes, to completely isotropic motions, are observed. The results suggest a model in which phenol inserts itself into the polymer backbone via nucleophilic attack. FTIR analysis does show phenol within exposed samples well

after drying, indicating that the molecule is bound to the polymer resin either via chemical reaction or steric hindrance. The deuterium NMR results are also consistent with covalent attachment [8]. The data thus far suggest that there is a combination of chemical reaction of the most vulnerable linkages within the coating as well as destruction due to swelling beyond the capability of the polymer making up the coating.

Materials and Methods

Chemicals

All chemicals were reagent grade and used without any further purification. The paint stripper solutions were prepared by weight according to the ratios in Table 1.

Table 1: Composition of Solvent Solutions

Solvent Formula	Weight Percent				
	methylene chloride	ethanol	water	phenol	Methocel ^b
Commercial Paint Stripper ^a	60.6	5.8	7.8	15.8	1.2
Methylene Chloride	100	---	---	---	---
Methylene Chloride and Phenol	79	---	---	21	---
Phenol and Ethanol	---	27	---	73	---
Methylene Chloride and Ethanol	91	9	---	---	---
Methylene Chloride, Ethanol, Water and Methocel	80	8	10	---	2
Methylene Chloride, Ethanol and Phenol	74	7	---	19	---
Methylene Chloride, Ethanol, Water, Phenol and Methocel	67	6	9	17	1
Methylene Chloride, Ethanol, Phenol and Methocel	73	7	---	19	1

^aAlso contains toluene (1.3%), sodium petroleum sulfonate (5.5%) and paraffin wax (1.9%),

^bMethocel added to emulsify into a single phase, with exception of methylene chloride, ethanol, and phenol solution.

The various formulations allowed for analysis of the different components of methylene chloride based paint strippers. Methocel is the trade name of hydroxypropyl methylcellulose.

Coatings

Currently employed military coatings were selected for this study. Two polyurethane topcoats were utilized as unsupported coatings (free films), with a film thickness of approximately five mils. The two military coatings used were MIL-PRF-85285 a two component high solids 2.8 VOC polyurethane topcoat and MIL-PRF-53039 single component aliphatic polyurethane CARC topcoat. Full formulation of the coatings can be found in Tables 2-3. The simplification of the otherwise complex coating system was selected to allow for ease of analysis. Resin binders and curing agents were combined as specified in Tables 4-5 to produce clear coat films of the

selected four military coatings. Each clear coat formulation was produced without pigments, additives, and solvents. In order to cast clear formulations to the required film thickness it was necessary to compound formulas to a workable spray application viscosity by adding the solvents contained in each formula in the proportions and thinning ratios specified. Elimination of entrapped air or solvents required either the addition of an antifoam agent or the readjustment of antifoam agent amounts or both. Antifoam agents used were those normally contained in each formula and were added in the proportions specified in Tables 4-5.

Full Coating Formulations:

Table 2: MIL-DTL-53039 Single Component Aliphatic Polyurethane CARC.

Raw Material	wt%	Raw Material	wt%
Polyurethane	31	Cobalt titanate spinel	0.4
Dispersant	1	Methyl isoamyl ketone	23.5
Rheology modifier	0.1	VM&P naptha	3.2
Flow modifier	<0.1	Xylene	1.4
Surfactant	0.1	n-Butyl acetate	1.3
Dibutyl tin dilaurate	0.5	Aromatic 100	1.3
Celite	18.5	Mineral spirits	1.2
Imsil	3.6	Propylene glycol	0.1
TiO ₂	9.5	Isobutyl ketone	0.1
Iron oxide hydrate	2.5	n-Butyl acid phosphate	0.1
Carbazole dioxazine violet	<0.1	Bentone	0.5

Table 3: MIL-PRF-85285 High Solids Polyurethane Topcoat.

Part A Raw Material	wt%	Part B Raw Material	wt%
Methyl N-propyl ketone	1	Polyurethane resin	43
Methyl N-amyl ketone	7	N-Butyl acetate	1.6
Anti-oxidant	0.3		
UV-absorber	0.5		
UV stabilizer	1		
Polyester solution #1	19.3		
Cellosolve acetyl butyrate	0.6		
Surfactant	0.1		
1% Thickener in xylene	0.2		
Thixotropic agent	0.2		
Dispersing agent	0.3		
TiO ₂	20.5		
Polyester solution #2	4.4		

Clear coat Formulations:

Table 4: MIL-DTL-53039 Single Component Aliphatic Polyurethane CARC.

Raw Material	wt%
Polyurethane	47.4
Dibutyl tin laurate	0.7

Dispersant	0.1
n-Butyl acetate	2
Methyl isoamyl ketone	38.2
Surfactant	0.2
Flow modifier	0.1
Rheology modifier	<0.1
VM&P naptha	4.8
Xylene	2.1
Aromatic 100	2
Mineral spirits	2
Propylene glycol	0.0
Isobutyl ketone	0.2
n-Butyl acid phosphate	0.2

Table 5: MIL-PRF-85285 High Solids Polyurethane Topcoat.

Part A Raw Material	wt%	Part B Raw Material	wt%
Polyester solution #1	24.4	Polyurethane resin	54.4
Polyester solution #2	5.5	N-Butyl acetate	2
Methyl N-amyl ketone	8.9		
Methyl N-propyl ketone	1.3		
Anti-oxidant	0.4		
UV absorber	0.6		
UV Stabilizer	1.3		
Cellosolve acetyl butyrate	0.8		
Surfactant	0.2		
1% Thickener in xylene	0.2		

The formulas were compounded to achieve continuous, anomaly-free films of the desired thickness by utilizing the identical rheology and flow modifiers specified in each formula. Clear films were created by spray application after altering the proportions of solvents, adhesion promoters, antifoamers, rheology, and flow modifiers utilized in each clear coating formulation as necessary. To help provide an intermediary between the two coatings a partial formulation was made. The partial formulations were the clear coats with only the pigments added. All coatings were prepared on release paper [8].

Sample Exposure

The samples for thermal analysis were exposed using the following method. Approximately two centimeter square coupons of each coating were cut and placed into individual scintillation vials. To each vial was added the respective solvent or solvent mixture (see Table 1) until the coating was completely covered (~10 mL). After exposure periods of two hours the liquid was decanted, rinsed with absolute ethanol and the coating allowed to air dry in the vial. A rinse with ethanol ensured that no remaining chemicals were adhered to the surface of the coating prior to analysis. Caution was taken to ensure the coating was completely dry before testing.

For vibrational spectroscopy the two centimeter square samples were exposed to individual solvents or solvent mixtures for times ranging from 15 minutes to two hours. The samples were then air dried thoroughly, for times ranging from two hours to two weeks, to reduce spectral contamination from residual solvent.

For confocal and contact angle analysis the samples followed the same procedure as the thermal except that they were exposed for twenty, forty and sixty minutes. This allows for a stepwise analysis of the paint stripper solutions method of attack on the coating. Then rinsed and dry for at least a day to ensure the coating was completely dry.

Experimental Methods

Differential Scanning Calorimetry (DSC)

Differential scanning calorimetry (DSC) was performed on a TA Instruments Q20 DSC with the DSC Refrigerated Cooling System (RCS) and a purge gas of nitrogen set to 50 mL/min.

Samples of approximately 1-2 mg were placed into TA Instrument Tzero Aluminum pans and an empty aluminum pan was used as reference. Samples were analyzed from -90 °C to 150 °C at 20 °C/min twice to demonstrate hysteresis. All data reported were taken from the second cycle. Glass transition temperatures (T_g) were found using TA Universal Analysis software.

Thermogravimetric Analysis (TGA)

Thermogravimetric analysis (TGA) was performed on a TA Instruments Q50 TGA using a platinum sample pan. The analysis was carried out in the presence of oxygen with breathing air used as the sample gas. Nitrogen was used as the purge gas for the balance. Data were recorded from ambient temperature to 700 °C at a 5 °C/min ramp. Plots of percent weight loss versus temperature were constructed to analyze the data.

Fourier Transformed Infrared Spectroscopy-Attenuated Total Reflectance (FTIR-ATR)

FTIR spectra were recorded on a Thermo Scientific Nicolet 6700 FTIR spectrometer equipped with a Smart Performer ATR attachment with a Germanium crystal at 32 scans. Spectra were recorded from 4000 – 500 cm⁻¹ with a resolution of 2 cm⁻¹, and were analyzed using the Nicolet OMNIC software suite.

Raman Spectrometry

Samples were analyzed using either a Nicolet Almega dispersive Raman spectrometer with 10x objective lens and 785 nm or 532 nm excitation laser; or a WiTec Alpha 500 confocal Raman spectrometer with 20x objective and 532 nm laser, at Brookhaven National Laboratory's Center for Functional Nanomaterials; the incident laser spot sizes of these instruments are less than 3 μm.

X-ray Photoelectron Spectroscopy (XPS)

X-ray photoelectron spectra were obtained using a VG ESCA-3 Mk. II system at ultra-high vacuum (10⁻⁹ torr). A pass energy of 20eV was used across 50 scans of the sample for each element, in combination with a magnesium K (alpha) anode operating at 120W. Spectra were calibrated using a reference value of 284.0 eV for adventitious carbon.

Scanning Electron Microscopy (SEM)

Micrographs were obtained using an FEI Helios Nanolab dual-beam scanning electron microscope with a secondary electron detector.

Contact Angle

Contact angle data were obtained using a VCA OptimaXE 2500 with the liquid drops of 2 μL . The surface free energy was determined using the Owens-Wendt theory with water and diiodomethane.

Confocal Laser Microscopy

Confocal laser microscopy was performed on an Olympus LEXT OLS4000 3D Measuring Laser Microscope with magnification from 108 to 2150. The roughness was calculated using the root mean theory.

Near Edge X-ray Absorption Fine Structure (NEXAFS)

NEXAFS spectroscopy was performed on beamline U7A at the National Synchrotron Light Source at Brookhaven National Laboratory to study the carbon and oxygen K edges of unexposed and exposed coatings. A grid bias voltage of 150V was used, which provides surface selectivity on the order of several nm, with a spot size of less than 1 mm^2 . Spectra were subsequently pre-/post-edge normalized prior to curve fitting and analysis. Custom software was written to calculate the dichroic ratio of each peak in each sample, utilizing data collected at 3 angles (20, 55, and 90 degrees relative to the sample). Hyperspectral acquisition of a large area sample (12x15mm) was done on the same beamline using the LARIAT detector.

Results and Discussion

Confocal and Scanning Electron Microscopy

In order to track the physical changes along the surface of the coating visible confocal microscopy was utilized. These changes can be tracked through visual inspection, micro scale, and also through surface roughness analysis. The inspection of fully formulated MIL-PRF-53039 shows very little to no change upon exposure to methylene chloride, as can be seen in Figure 1. Upon exposure to methylene chloride and ethanol the same results was seen for fully formulated MIL-PRF-53039. This trend was observed for the partially formulated MIL-PRF-53039 as well as both the partially and fully formulated MIL-PRF-85285 coatings exposed to methylene chloride and methylene chloride and ethanol. Exposure of the coatings to solutions containing phenol resulted in significant visible changes, Figure 2. The development of porosity and larger holes along with surface blistering implies that chemical degradation has occurred. The observations of methylene chloride, methylene chloride and ethanol and phenol containing solutions were confirmed using SEM to analyze the nanoscale changes of the coatings. The results were the same as the confocal imaging with significant degradation seen only for the coatings exposed to solutions containing phenol.

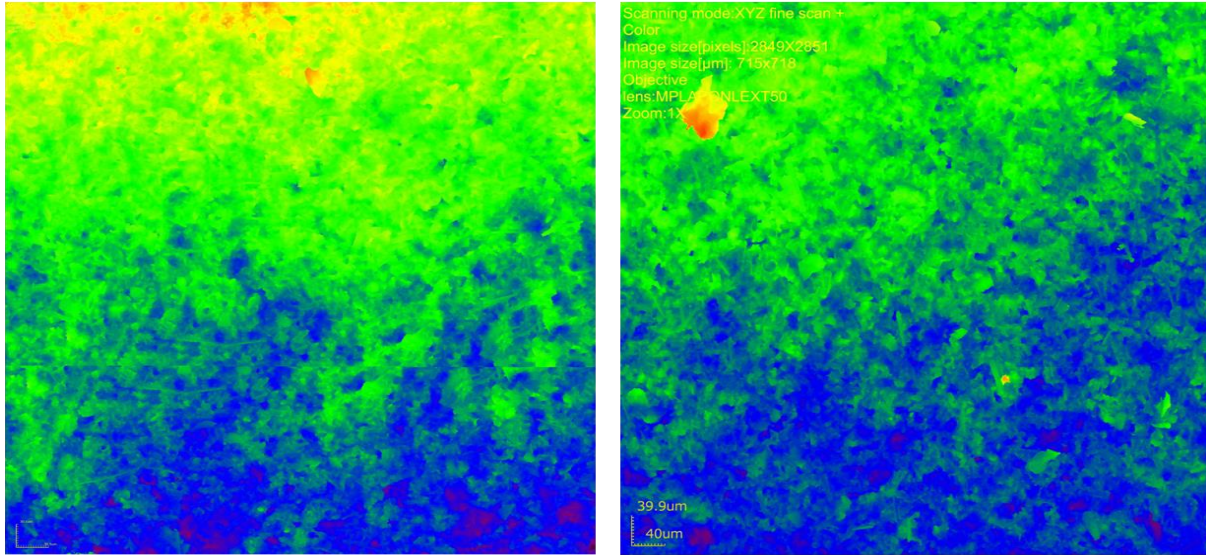


Figure 1: Confocal false color three dimensional images of unexposed MIL-PRF-53039, left, and MIL-PRF-53039 exposed to methylene chloride for sixty minutes, right.

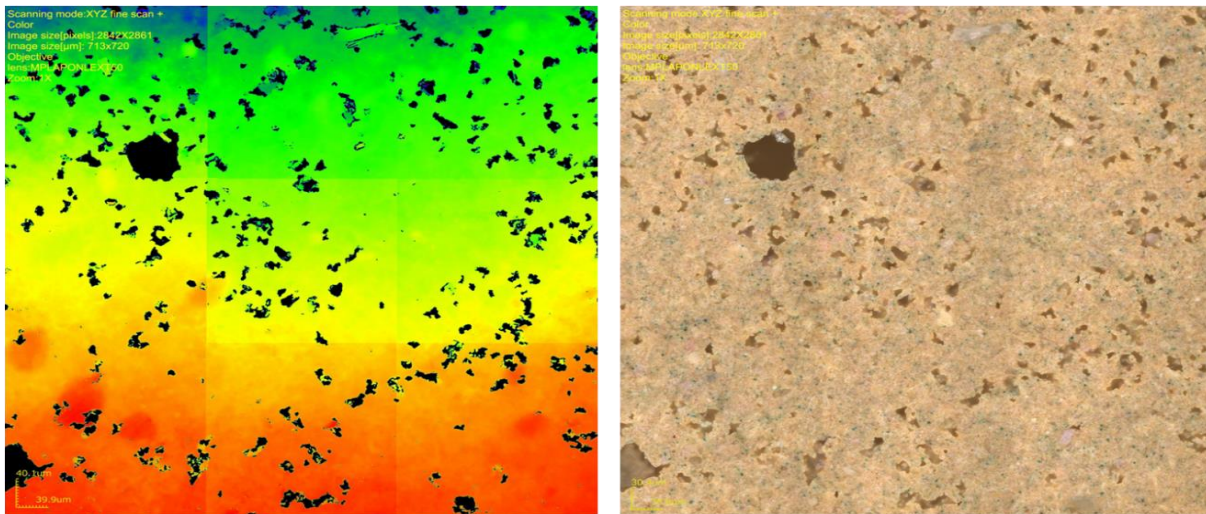


Figure 2: Confocal false color three dimensional and color image of MIL-PRF-53039 exposed to methylene chloride, ethanol, water, phenol for forty minutes.

The visible degradation in coatings exposed to phenol correlates with previous work that showed that phenol was the main agent of degradation [8]. An interesting development occurred upon examination of the coatings exposed to methylene chloride, ethanol, water and methocel. The development of a sporadic film was noticed on these coatings, Figure 3. The film was observed on both MIL-PRF-53039 and MIL-PRF-85285. Upon further analysis the presents of “bubbles/blisters” in the film were observed.

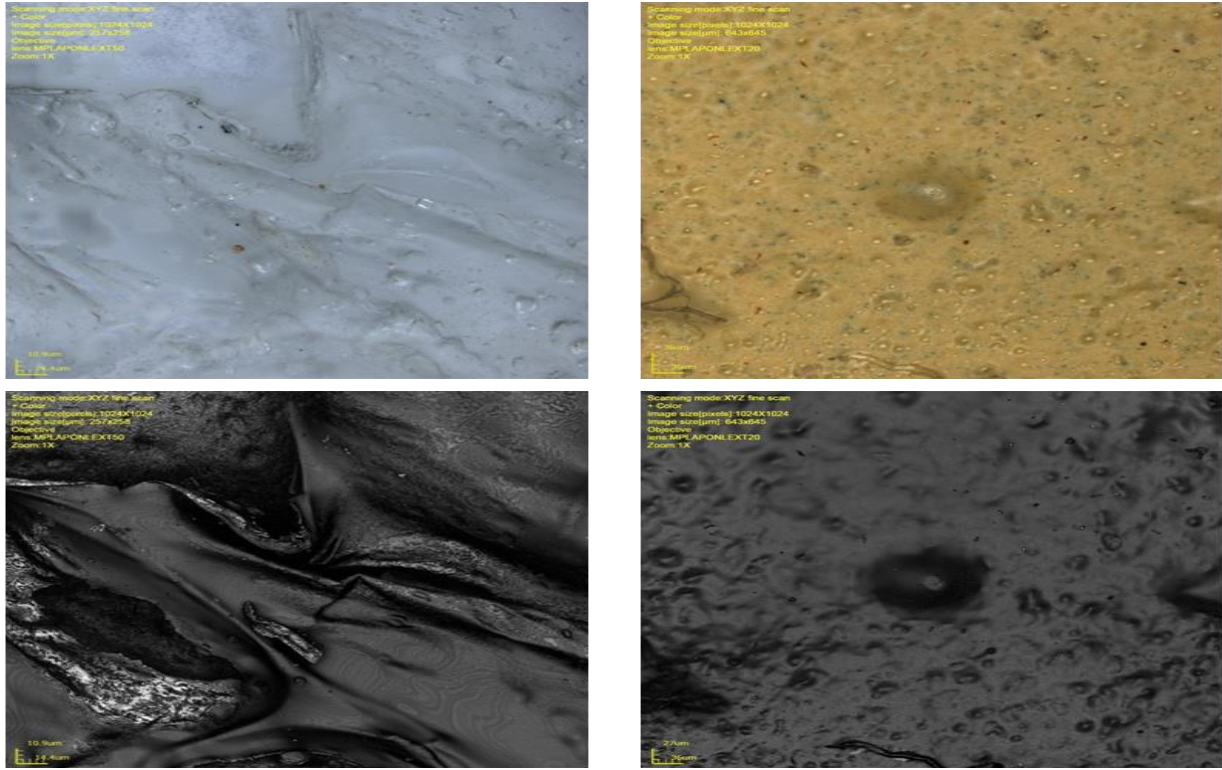


Figure 3: Confocal images of film deposition on MIL-PRF-85825, left side, and MIL-PRF-53039, right side after exposure to methylene chloride/ethanol/water.

The presence of this film was also found on all coatings when exposed to the methylene chloride, ethanol, water, phenol and methocel. SEM images were taken to confirm that a film had formed on the surface of the coatings. The images seen in Figure 4 show a heterogeneous film deposition on MIL-PRF-53039.

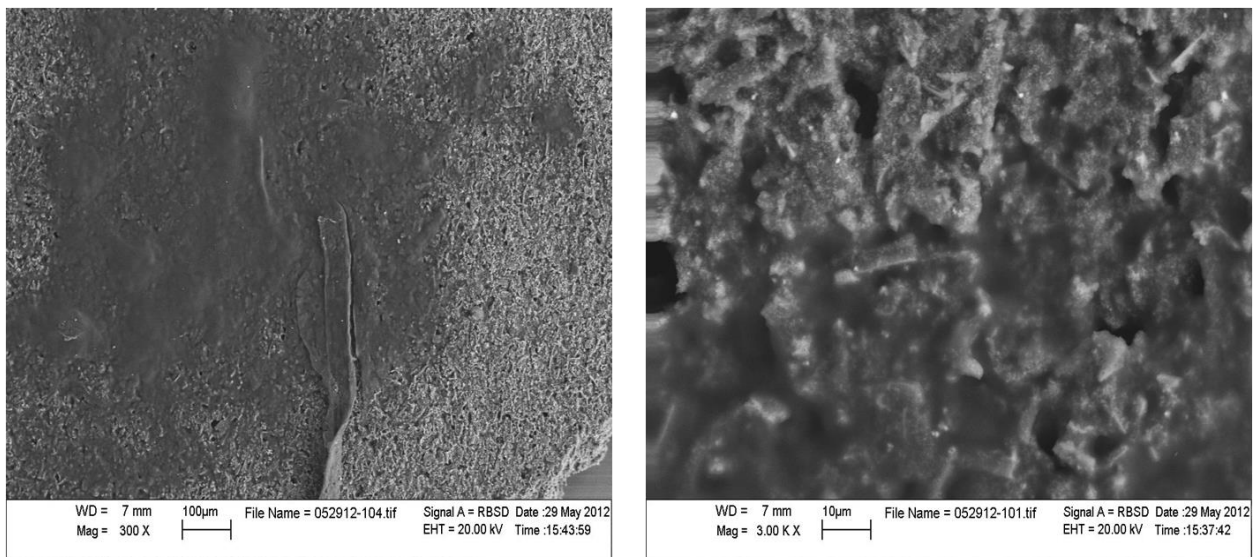


Figure 4: SEM images of MIL-PRF-53039 exposed to methylene chloride, ethanol, water and methocel

The films appearance on only the coating containing water and methocel indicates that one of these is responsible for the film formation. Methocel is the trade name for hydroxypropyl methyl cellulose which acts as an emulsifying agent for the paint stripper [9]. Methocel is a polymer and could be the film that is seen on the coatings. In order to determine the effects and presence of the film the methylene chloride/ethanol/phenol/methocel solution and the methylene chloride/ethanol/phenol solution was made and additional tests were performed. Confocal images taken of the coatings exposed to methylene chloride/ethanol/phenol showed no film deposition. On the coatings exposed to methylene chloride/ethanol/phenol/methocel film deposition was found indicating that the film is methocel deposition. Further analysis was done to confirm that methocel is depositing on the surface of the coating.

Spectroscopy

To determine if the film seen on the surface is methocel and if it may affect the degradation of the coating a variety of spectroscopy techniques was utilized. FTIR-ATR spectra were obtained for the samples that were exposed to the solutions containing methocel (Table 1). The spectrum of pure methocel was obtained as well as one of the unexposed coating. By overlaying these three spectra it can be determined if methocel is on the surface of the coating, Figure 5.

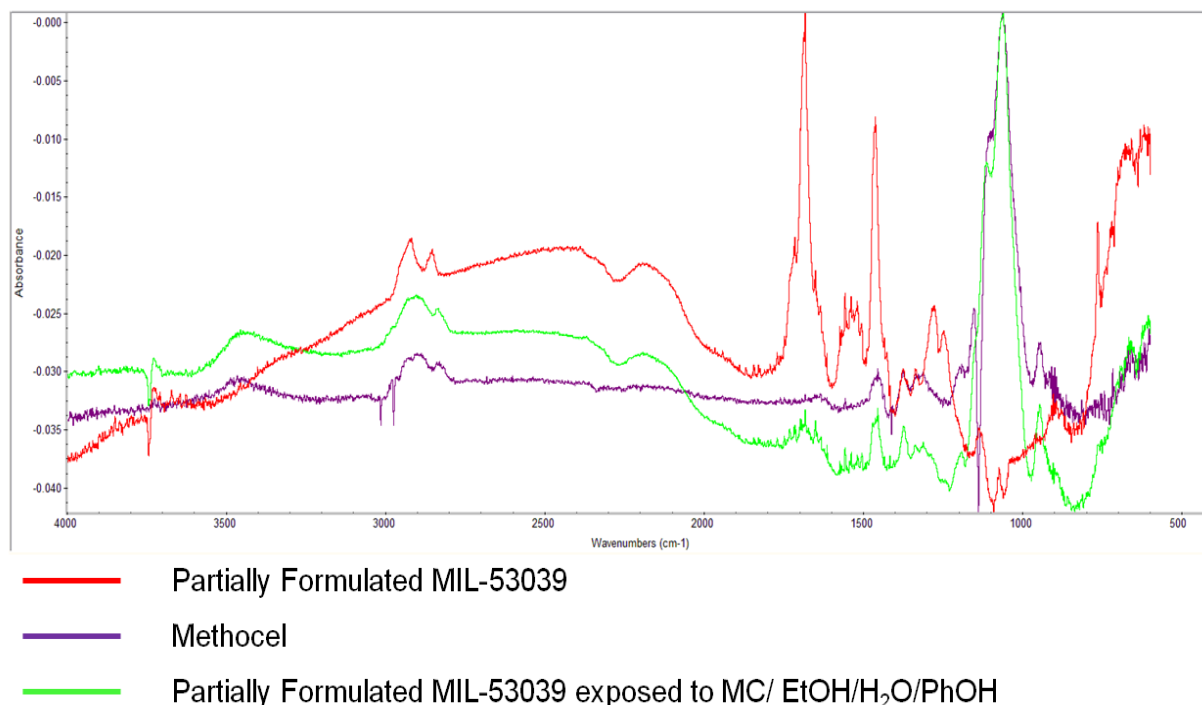


Figure 5: FTIR-ATR Comparison of partially formulated MIL-PRF-53039

The purple spectrum of methocel has a large peak at 1060 cm^{-1} , indicative of a carbon oxygen single bond, with only a few other peaks present. The spectrum of the partially formulated MIL-PRF-53039 exposed to methylene chloride, ethanol, water, phenol and methocel also has a large peak at 1060 cm^{-1} . The reduced peak signals at 1460 cm^{-1} and 1680 cm^{-1} in the exposed coating and the lack of any peak at 1060 cm^{-1} in the spectrum of the unexposed coating further implies

that methocel has deposited on the surface. FTIR-ATR using a germanium crystal only penetrates approximately 0.65 μm [10]. Knowing the penetration depth and that peaks from the unexposed coating are still seen in the spectrum of the exposed coating leads to an important observation. The deposited methocel layer is less than 0.65 μm and/or the film deposition is patchy. The shallow depth of the film reveals that the methocel is present only on the surface and doesn't penetrate the coating. While FTIR-ATR spectra show compelling evidence for methocel deposition on the coatings Raman microscopy was done to confirm and further analysis methocels presence.

An approach similar to the FTIR-ATR was used. The Raman spectrum of exposed coatings, one shown in figure 6, was compared to the spectrum of methocel. As seen in the FTIR-ATR the two spectra have similar features with a large peak seen at 2900 cm^{-1} and the smaller peaks

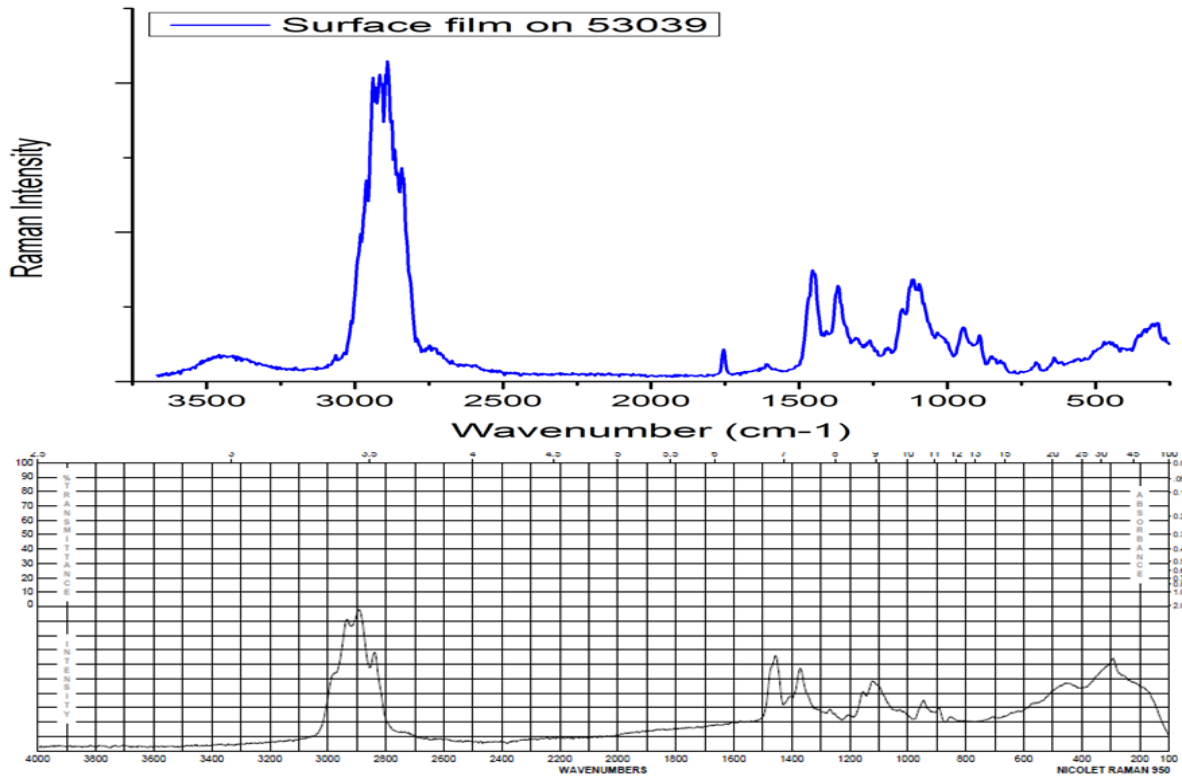


Figure 6: Raman spectra of Methocel and MIL-PRF-53039 with film on surface

seen near 1400 and 1100 cm^{-1} . The spectra are slightly different especially the small peak at 1750 cm^{-1} indicating that the methocel doesn't entirely cover the surface. Specifically some polyurethane spectrum (C=O) remains visible, the same as the FTIR-ATR. Careful surface analysis of the exposed coatings reveals a near-perfect match for methocel thickness $< 1 \mu\text{m}$.

X-Ray Photoelectron Spectroscopy (XPS) analysis of the coatings exposed to the paint stripper solutions with methocel allows for a closer look at the development of the C-O peak and the disappearance of the C=O seen in both the FTIR-ATR and Raman. In the middle spectrum of

Figure 7, C1s shows that methocel obscures the C=O response, and increases C-C relative to C-O. Incomplete attenuation of C=O indicates incomplete coverage of the methocel film on the coating.

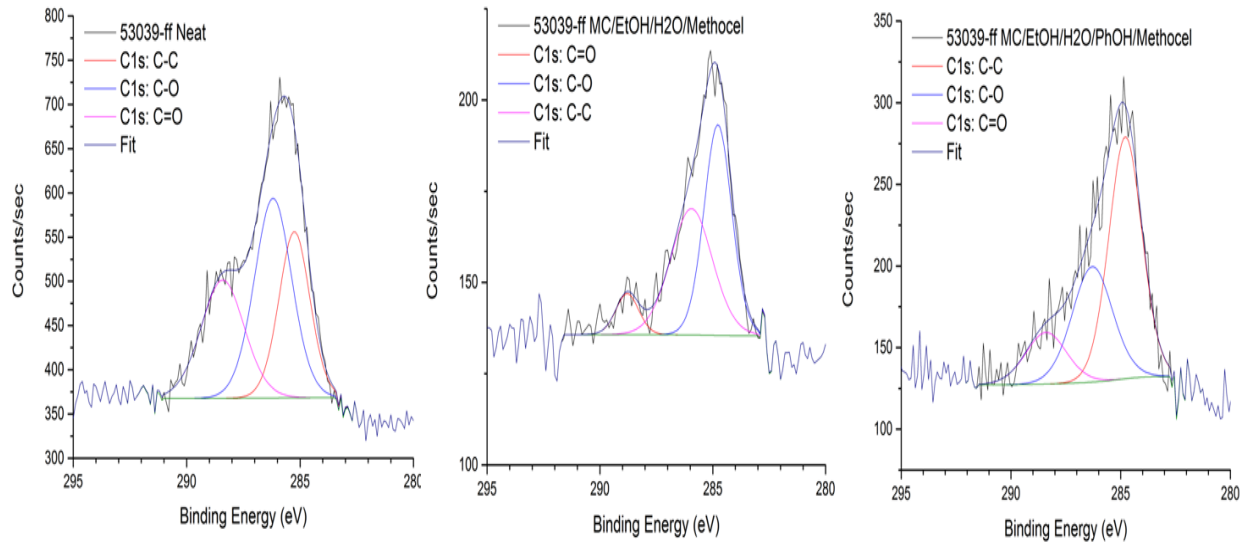


Figure 7: XPS spectra of MIL-PRF-53039

Stronger C=O response in coating exposed to phenol, vs. coating with methocel but without phenol, is indicative of coating degradation and subsequent film breach. This exposes the coating beneath, which is seen in the spectrum. The coating degradation was seen on the SEM and confocal images and also correlates with data in previous work [8]. The XPS data show that methocel deposits on the surface of the coating and that even though it covers up some aspects degradation can still be seen with the solutions containing phenol.

NEXAFS analysis on select coatings was conducted and analyzed. Software for hyperspectral analysis from this detector was used to select regions of interest in each sample for further curve fitting and analysis. Black and white images of the sample were created from the integrated area of the peaks of interest. Absorption peak values for NEXAFS spectroscopy are not as ubiquitous as for XPS, so efforts were taken to use systems which best compared to those analyzed as reference data. An X-ray absorption transition is described in general; as C1s- π^* (C=C) for simplicity, we will concisely describe such a transition as C=C π^* . Curve fitting was performed over a range from 284 eV, to capture the pre-edge baseline, to 302.5 eV. The ionization potential of carbon was modeled as an exponential step at approximately 290 eV with a width of 1 eV or less. Given the different chemistries involved in the coating a small degree of flexibility in the fit to account for variations in chemistry, even though the position and width were very consistent across samples. The pre/post edge correction process used performs two tasks. First, the pre-edge is subtracted to remove the overall background, providing the correct intensity of the spectrum. The post-edge correction, which sets the long-tail end of the data to an intensity of 1, provides normalization of the data. Accordingly, a corrected spectrum with a higher overall integrated area shows a somewhat higher density of oscillating atoms within a

region of interest than another spectrum with a lower integrated area. Utilizing the basis of normalization for the obtained spectra, the regions of decreased intensity overall correspond to more porous areas of the coating, which demonstrates that the coating is heterogeneously porous over the dimensions of the areas of interest (500 x 500 um).

Spectra were obtained for each coating system prior to exposure. Spectra presented here come from measurements taken at 55 degrees, which is the “magic angle” to eliminate orientation effects, as was remarked upon for solid-state NMR in a previous report. It is immediately apparent that the coating surface is chemically heterogeneous, with differing concentrations of some moieties at different positions.

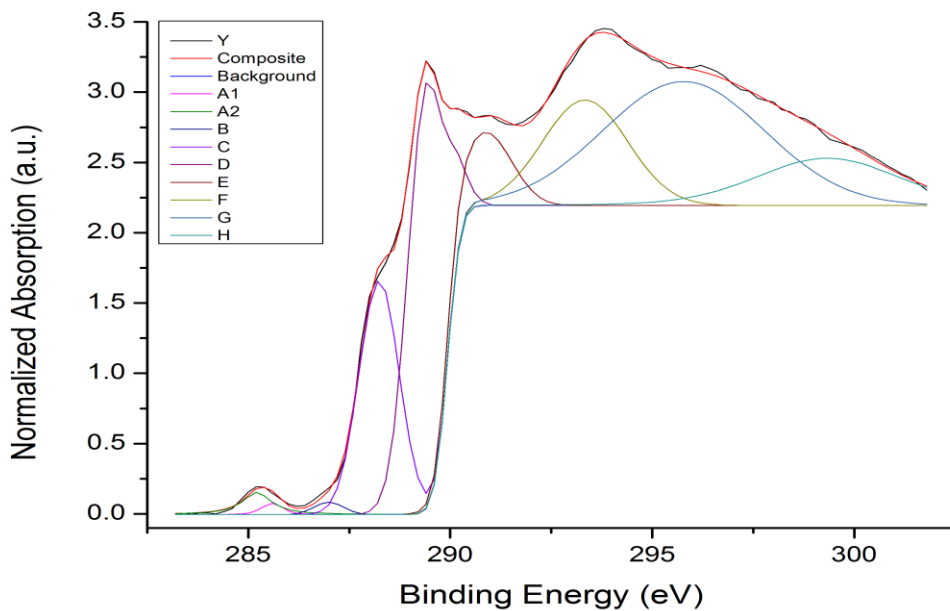


Figure 8: NEXAFS C K-edge spectrum of unexposed, fully-formulated MIL-PRF-85285 (blue color), top surface.

The top or outward facing side of the coating system was analyzed first. Given the aliphatic nature of MIL-PRF-85285, the peak exhibited by the outward-facing surface shown in Figure 8 and Table 6 for C1s- π^* C=C at 285.4 eV, peak A, must be attributed to an additive in the polymer. This is due to the presence of UV stabilizing compounds, which might consist of a benzophenone-based molecule or similar. A single curve fit for this peak is too broad for this technique, with the full width half maximum (FWHM) of 0.8 eV. Fitting two peaks at 285.2 and 285.7 eV, dubbed A1 and A2, results in somewhat more reasonable FWHM values, ~0.6 eV, for a peak at this binding energy. Since the fitted peaks are dissimilar in area, with A1 generally being larger than A2, we are confident in this assignment. The small peak at 286.7 eV (B) corroborates the prediction of a molecule resembling benzophenone, as it corresponds to the transition seen in a carbonyl which links two aromatic rings. The peak, C, in the carbon K edge spectrum at 288 eV C-H σ^* absorptions from the long chains of the polyisocyanates and

polyesters [11]. The 289.4 eV, peak D, are related to C=O π^* absorptions due to the polyisocyanates. This peak fits well for the types of urea linkages seen at the heart of many structures commonly employed in the formation of polyisocyanates from HDI [12]. The peak at 290.7 eV, E, appears to be the aggregate of several peaks: the C=O π^* transition for urethanes, the C-N σ^* transition from the same, and the C=C $2\pi^*$ transition. The literature states that the carbonyl peak should be closer to 290 eV however; this single peak is overly broad for this assignment. Obtaining the proper fit information for the ionization edge area between 290 and 291 eV was a significant challenge, this lead to the conclusion to under-fit the curve [13]. Further peaks at ~293, ~296, and ~299 eV (F, G, H) are σ^* transitions which relate to C-C, C-C/C-O, and C-C, respectively [14]. The positions and assignments of these peaks are presented in Table 6.

Table 6: Labels and assignments of NEXAFS C K-edge peak fits

	<i>Binding Energy (eV)</i>	<i>Structure</i>
A	285.2, 285.7	C=C aromatic π^*
B	286.8	C=O π^* conjugated systems
C	288	C-H σ^*
D	289.5	C=O π^*
E	290.7	C=O π^* , C-N σ^* , C=C $2\pi^*$
F	293	σ^* (C-C)
G	296	σ^* (C-C/C-O)
H	299	σ^* (C-C)

The substrate-facing or bottom side of the coating was also analyzed in order to compare the top. In Figure 9, we show the substrate-facing side of the coating, following removal from release paper.

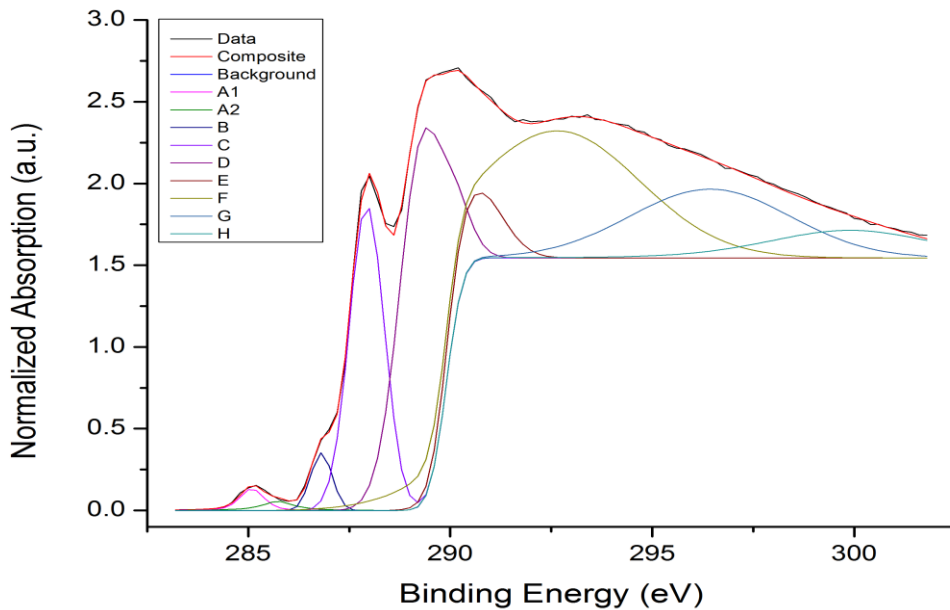


Figure 9: NEXAFS C K-edge spectrum of unexposed, fully-formulated MIL-PRF-85285 (blue color), bottom surface.

The A peaks are appreciably stronger at the bottom surface than on the top surface, by roughly 40%. As expected with the increase in aromatics, the A peaks, peak B shows an increase in intensity. Peak C is much stronger than at the top surface, leading it to become distinct, and peaks D and E are now roughly equal in spectral height. The σ^* peak F is less distinct here than on the top surface, and peak G is largely indistinct. Peaks C through G are mostly related to the polymer chain and suggest that different moieties have segregated to the top and bottom surfaces. Figure 10 presents the NEXAFS spectrum of the top surface of clear-formulated MIL-PRF-85285 which contains no pigmentation or fillers.

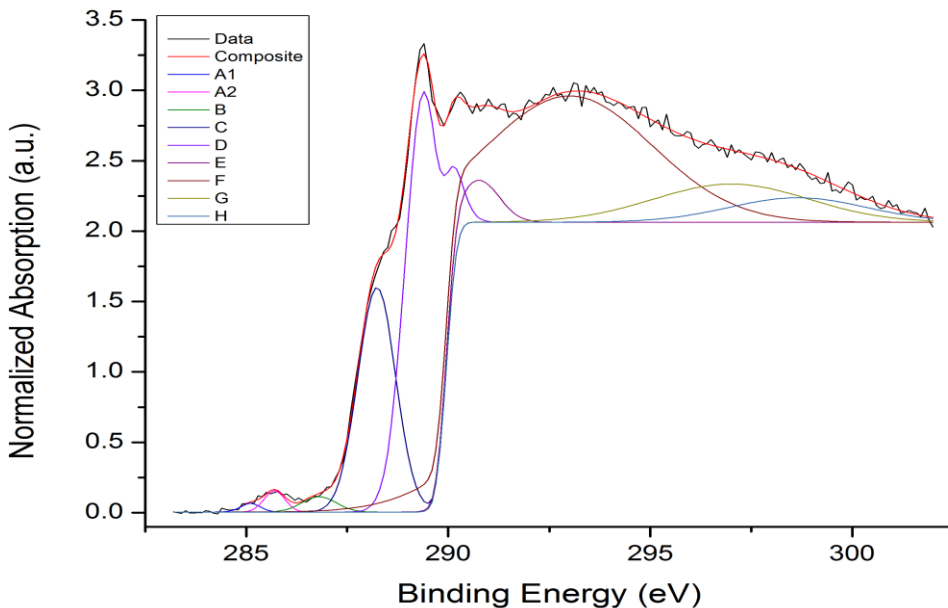


Figure 10: NEXAFS C K-edge spectrum of unexposed, clear-formulated MIL-PRF-85285, top surface.

While the structure of the spectrum is similar to the pigmented system, the parameters for peak fits demonstrate that there are major differences. The C=C π^* aromatic peak at 285.4 eV remains, but whereas in the first spectrum the lower-energy peak, A1, was larger than the higher-energy peak, A2. The opposite is now true, and the fit quality is poorer. Peak B remains largely unaffected. The change in the A peaks leads to the conclusion that in addition to indicating a stabilizer, the aromatic peaks are also related to the pigmentation used. Peaks C and D remain as before, as expected since they are from components of the resin itself. Peak E increases relative to the adjacent carbonyl, but this occurs heterogeneously across the surface; some areas show a low spectral feature at this binding energy. Further heterogeneity is seen in peaks F, G, and H. This may suggest that creating a homogenous clear coating of the coating is more problematic than initially thought.

Figure 11 presents the NEXAFS spectrum of the bottom surface of clear-formulated MIL-PRF-85285 which contains no pigmentation or fillers. Looking at the spectrum it is immediately obvious that the surface of this sample does not compare favorably to its pigmented counterpart.

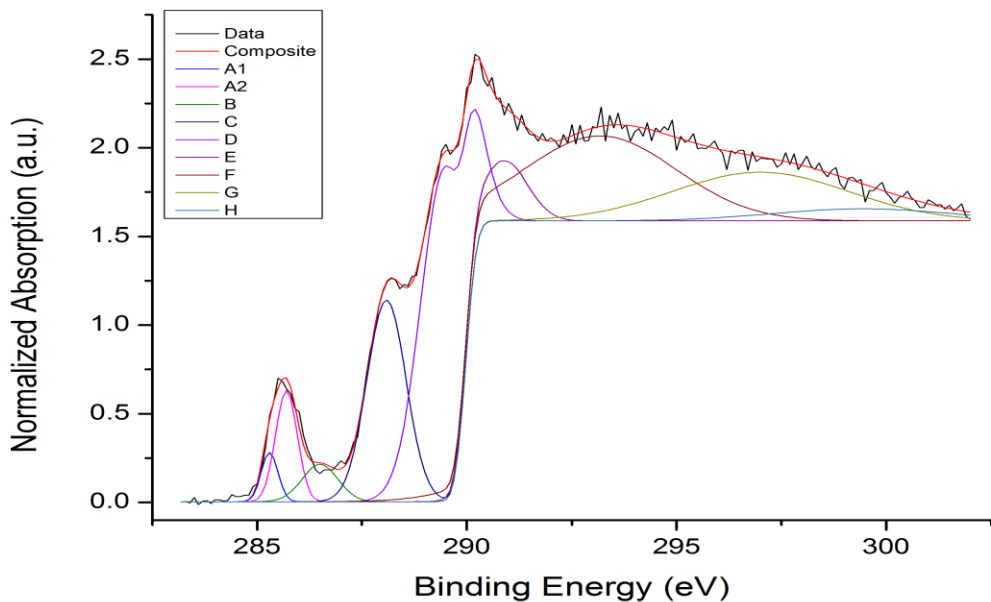


Figure 11: NEXAFS C K-edge spectrum of unexposed, clear-formulated MIL-PRF-85285, bottom surface.

The A peaks are much larger indicating that the amount of aromatic carbon at the surface is 2-3 times higher, and is much more heterogeneously distributed. Peak B's overall intensity is higher but looks diminished by the large A peaks. This could be an unknown source of aromatic material in the resin system. The other most significant change to this spectrum is the depletion of C=O peak, D. It is possible that the PVF release paper used is specifically repulsive to carbonyl interaction, and attractive to aromatics, hence causing localized aggregation and depletion at the surface.

Coatings were analyzed after a droplet of the paint stripper solvent component was applied to the surface and subsequently dried. Methylene chloride was applied to the coating and analyzed. The black and white image of this exposure, selecting for the presence of C=C, is shown in Figure 12. Which clearly demonstrates the location of the center of the droplet and the maximum diameter of exposure.

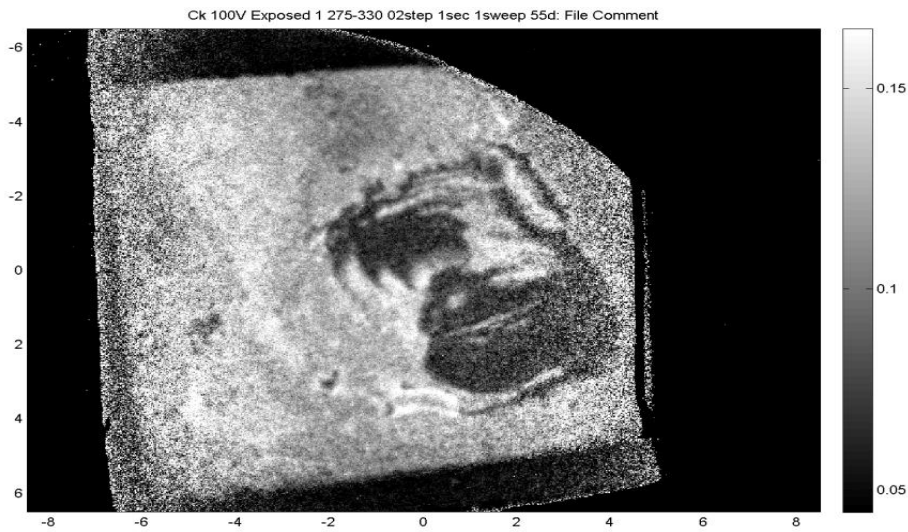


Figure 12: Black and white hyperspectral image of MC-exposed, fully-formulated MIL-PRF-85285, top surface, with brightness linked to C=C π^* peak area.

Spectra at the far edges of the sample are consistent with the unexposed sample, showing that the solvent did not diffuse to these regions. Broadly, there are two regimes of interest due to exposure: the center of the droplet, and the halo around the droplet. Analysis of these two regions reveals markedly different spectra. In Figure 13, the NEXAFS spectrum is shown from the application of methylene chloride to the surface.

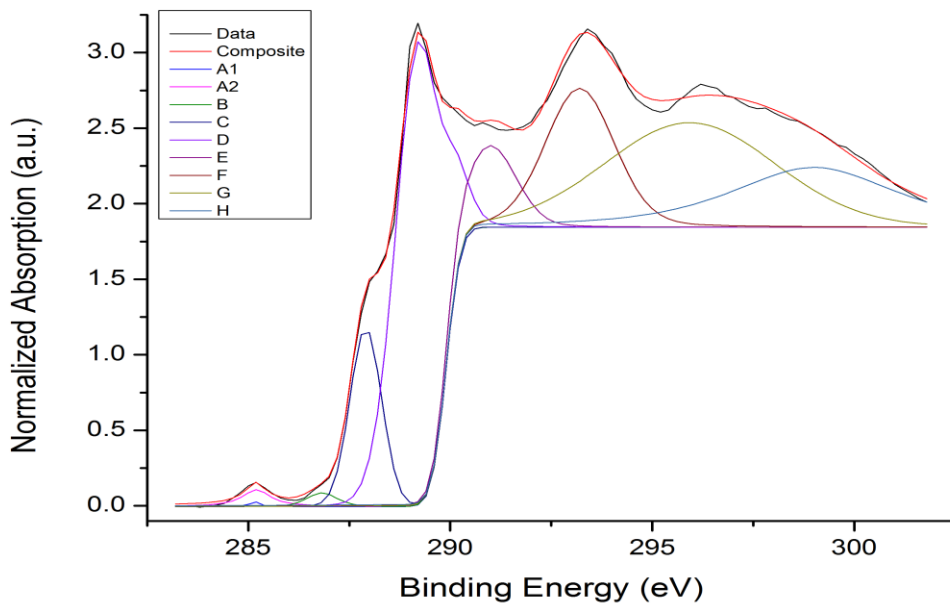


Figure 13: NEXAFS C K-edge spectrum of MC-exposed, fully-formulated MIL-PRF-85285, top surface, within the area of the methylene chloride droplet.

In the center, the A peaks indicating aromatic C=C have decreased. It appears that the aromatic-based additive has been solubilized and displaced. The amount of peak C decreases slightly relative to the amount of peak D, and peak G becomes somewhat less pronounced. The changes in these peaks suggest an effect on the polymer chains. Peak D shows a small shift to lower binding energy by about 150 meV. The small changes to the peaks are within the experimental error of the instrument, which could be due to changes in the local steric environment about the carbonyl as a result of polymer swelling and rearrangement. The intensity of peak E drops slightly, particularly as relating to its contribution around 290.1 eV.

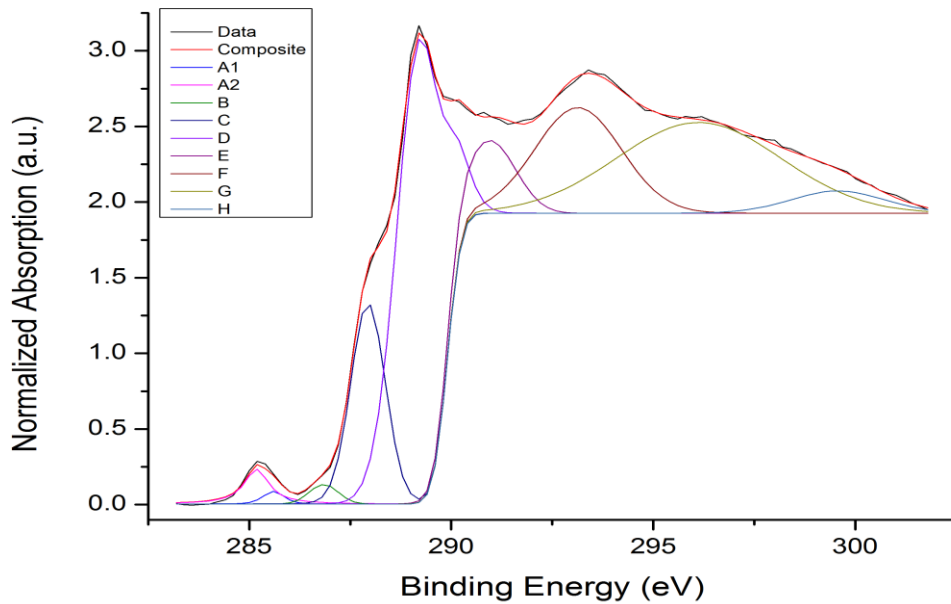


Figure 14: NEXAFS C K-edge spectrum of MC-exposed, fully-formulated MIL-PRF-85285, top surface, in the halo-like ring around the outer perimeter of the methylene chloride droplet.

In the halo region of Figure 12 the overall intensity of peak A increases by roughly 50%, Figure 14. This reveals that the aromatic additive depleted from the center of the droplet has been redeposited here. Previously, this group had proposed a model of methylene chloride solvation of the carbonyl in polyurethane, with a subsequent chain rearrangement as a result of increased polymer segmental dynamics. Based on changes to peaks C and G, we can conclude that the solvent has had some effect on polymer chain configuration, validating that model. Based on the analysis of several regions of interest, the overall intensity of the spectrum is decreased by exposure, which suggests that the polymer swelling and relaxation leads to a new configuration at a slightly lower overall density of chains at the surface. With only a minimal effect on surface energy seen from this exposure, we may conclude that these chain effects play a small role in hydrophobicity and surface interactions.

Figure 15 provides the same black and white image corresponding to peak A for exposure on the bottom surface of the coating.

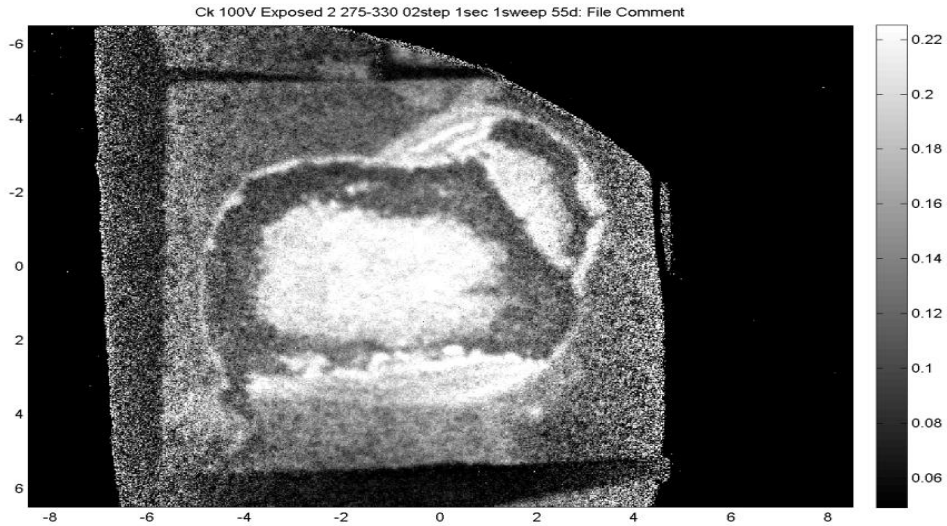


Figure 15: Black and white hyperspectral image of MC-exposed, fully-formulated MIL-PRF-85285, bottom surface, with brightness linked to C=C π^* peak area.

In Figure 16, we show the spectrum following exposure within the area of the droplet, while Figure 17 provides the spectrum of the ring around the droplet center, seen as a darker region in the image.

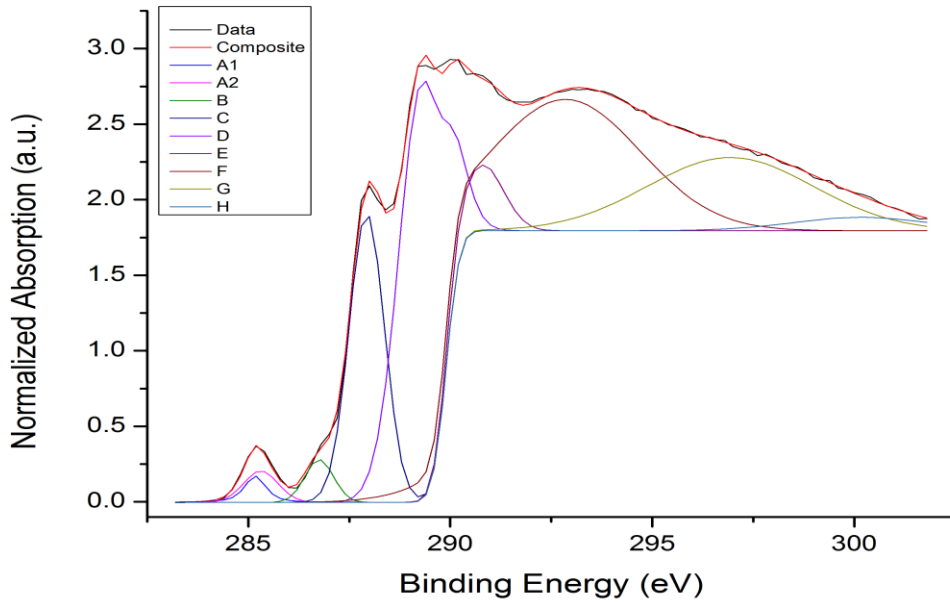


Figure 16: NEXAFS C K-edge spectrum of MC-exposed, fully-formulated MIL-PRF-85285, bottom surface, within the area of the methylene chloride droplet.

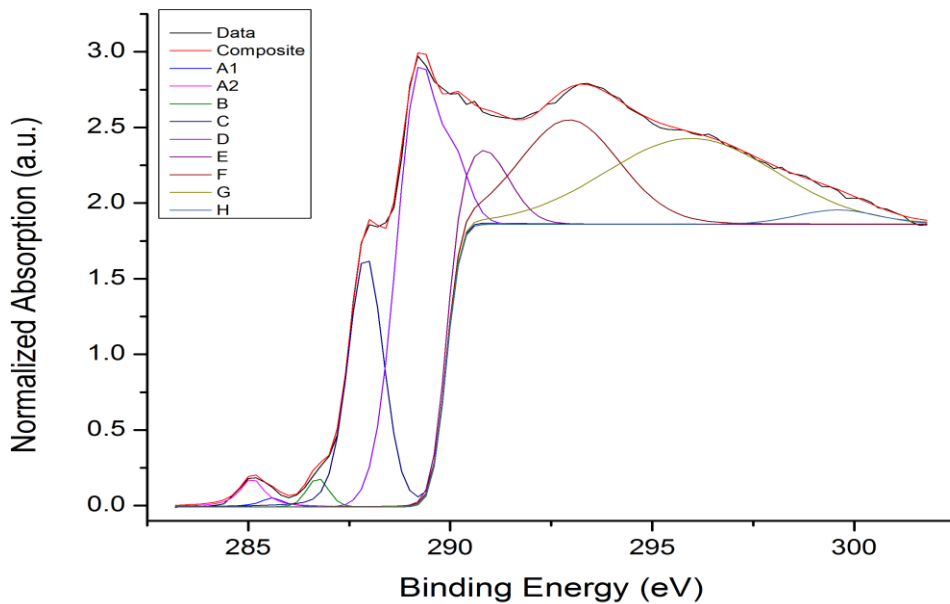


Figure 17: NEXAFS C K-edge spectrum of MC-exposed, fully-formulated MIL-PRF-85285, bottom surface, in the halo-like ring around the outer perimeter of the methylene chloride droplet.

Unlike the top coating, the concentration of C=C increases at the center of the droplet. Peak B shows some decrease in both the droplet and ring. The intensity of peak C is somewhat negatively impacted relative to the height of peak D, and in the ring region peak G is less distinctive, which again speaks to a change in polymer chain configuration. Peaks E and D remain in roughly their original proportion in the droplet region, but peak D is diminished in the ring around the sample.

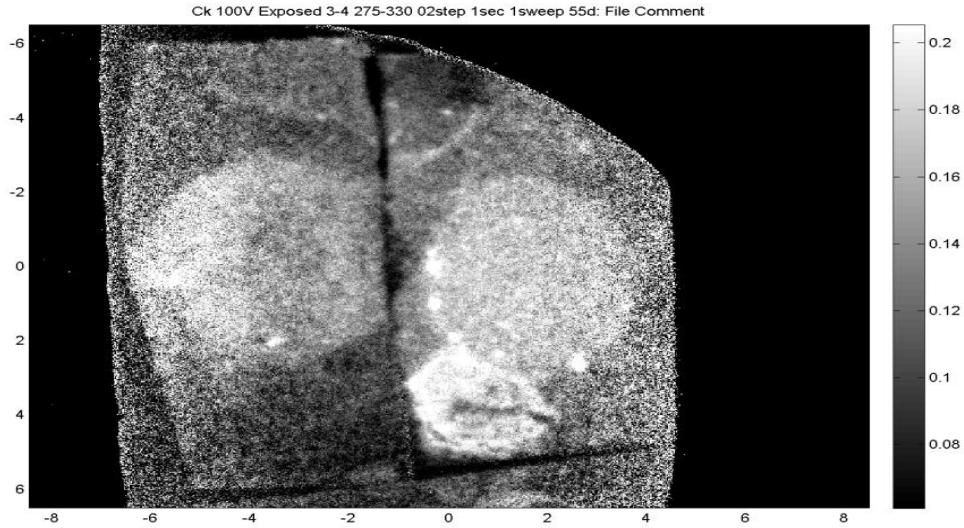


Figure 18: Black and white hyperspectral image of Phenol/water-exposed, fully-formulated MIL-PRF-85285, bottom surface (left) and top surface (right), with brightness linked to $C=C \pi^*$ peak area.

In Figure 18, we present a black and white image of both the bottom, left, and top, right, surfaces of coating 85285 after exposure by a droplet of liquid phenol, 91% Phenol, 9% H_2O , with coloration linked to the area of peak A. Figure 19 and Figure 20 show the spectra of these droplet regions as taken from the top and bottom surfaces, respectively.

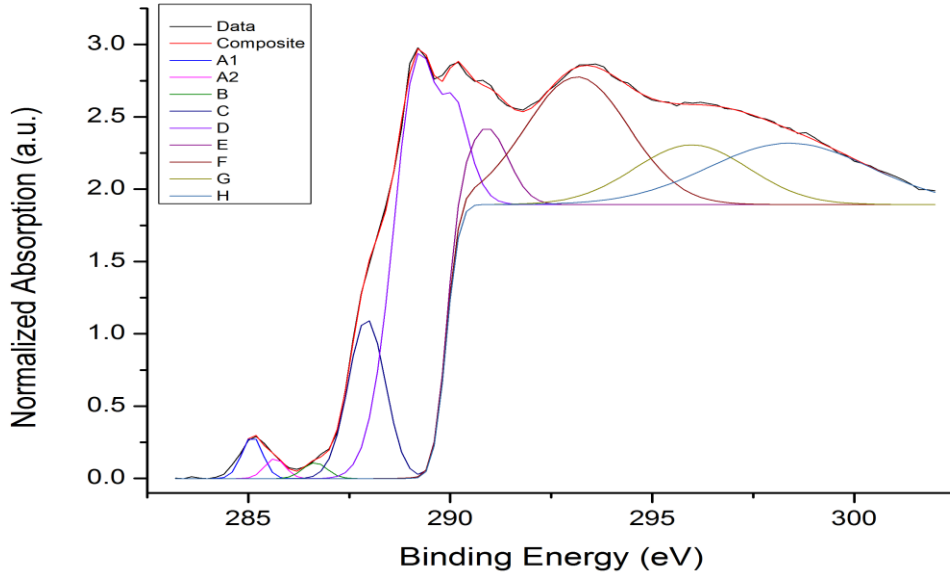


Figure 19: NEXAFS C K-edge spectrum of Phenol/ H_2O -exposed, fully-formulated MIL-PRF-85285, top surface, in the region of the droplet.

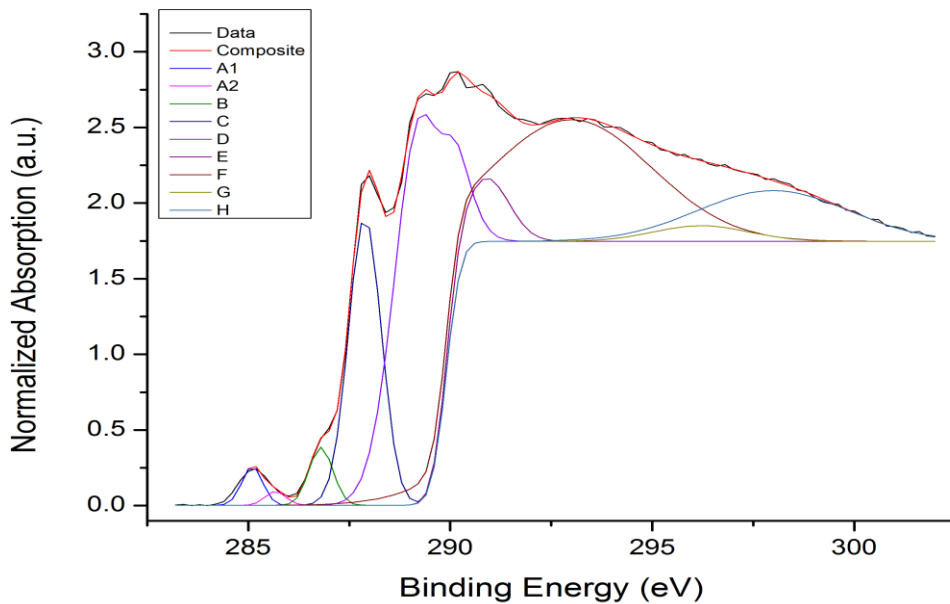


Figure 20: NEXAFS C K-edge spectrum of Phenol/H₂O-exposed, fully-formulated MIL-PRF-85285, bottom surface, in the region of the droplet.

Small changes occur in peak A and significant changes occur in peak E, both of which may be attributed to aromatic π^* transitions, $1\pi^*$ and $2\pi^*$, respectively. Through these changes, we confirm that part of peak E relates to the presence of aromatics in the coating.

From our thermal analyses, we know that methylene chloride and phenol in combination serve to produce a significant decrease in the T_g of the coating see Table 10. Having also established that the presence of methocel produces a conformal coating with a depth that X-rays may not penetrate, we have analyzed the surfaces of this coating after exposure to methylene chloride/ethanol/phenol.

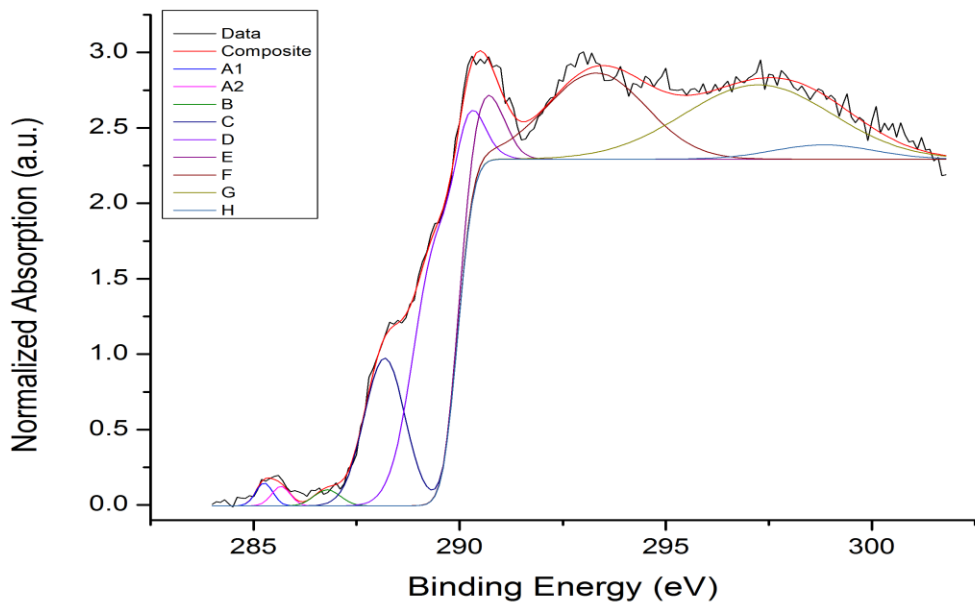


Figure 21: NEXAFS C K-edge spectrum of methylene chloride/ethanol/phenol-exposed, fully-formulated MIL-PRF-85285, top surface.

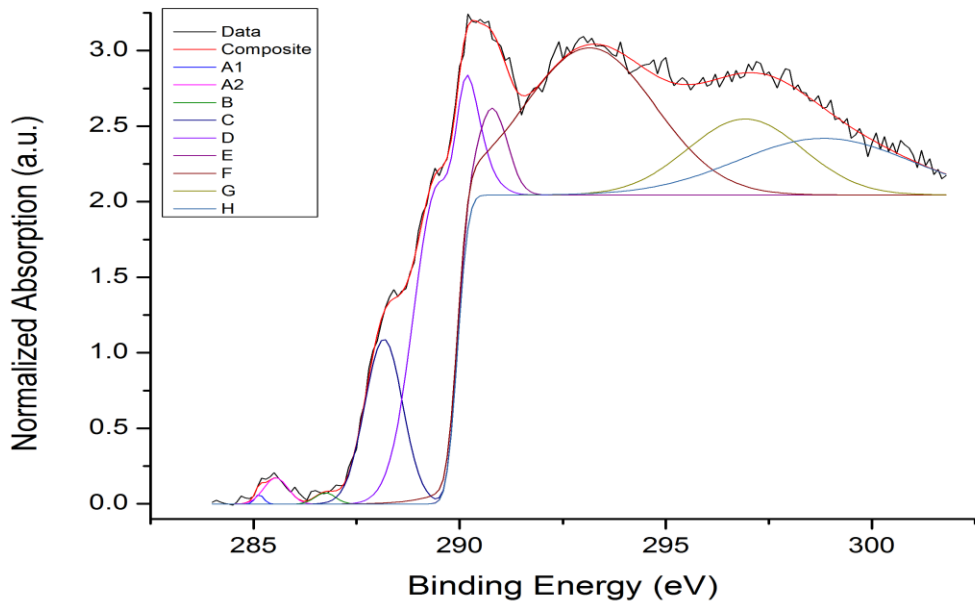


Figure 22: NEXAFS C K-edge spectrum of methylene chloride/ethanol/phenol-exposed, fully-formulated MIL-PRF-85285, bottom surface.

These spectra, seen in Figure 21 and Figure 22, demonstrate the persistent effects of these solvents due to exposure. Previous work for this project shows that significant amounts of phenol remain in the sample, giving it a purple tint and persistent odor for years after exposure.

[8]. There is no measurable increase in the peaks at region A, which is surprising given the aforementioned phenol retention and the previous results. Peak E increases dramatically in these spectra, such that it is the dominant feature at and around the ionization potential step. The fitted spectrum has a peculiar appearance, while the center of peak D occurs as usual at 289.4 eV. The peak however is no longer more intense than the ionization edge, thus giving the remainder of the peak the appearance of a second maximum at 290.2 eV. Additionally, the proportional change in height of the ionization edge makes it difficult to remain consistent with regards to the significance of peak areas from previous samples. The large increase of peak E is difficult to explain based on our initial definitions since peaks in region A are expected to increase with phenol. The small increase seen in the phenol/water exposed coating's spectrum implies that phenol has little effect on peak A. The other evidence of phenol persistence in the previous report and thermal analyses leads to the conclusion that increases in peak E being due to degradation or interaction of phenol with the coating.

While methylene chloride was previously shown to cause no significant change which could be resolved through Raman, ATR-FTIR, or large-area XPS, a more focused study with an imaging technique has revealed that there are subtle changes. With adequate lateral resolution of an exposed region, we can see that coating additives distribution is affected by the addition of solvent. Further, the solvent extraction of such additives during exposure could certainly contribute to increasing the rate of infiltration of paint removing solvents. Methylene chloride has also been demonstrated to lead to polymer chain rearrangement and reordering, which is behavior consistent with the model of carbonyl solvation and inter-chain cross-linkage separation previously posited [8]. While the degree of order induced is low compared to many other measured systems, the values are not unusual for a bulk system [15]. The changes to ordering differ between the outward-facing and substrate-facing surfaces of the coating, suggesting appreciably different near-surface molecular morphologies in addition to the observed chemical compositions. The varied behavior of these surfaces is indicative of an engineered coating with appropriate surface-segregating functionalities. While components have been suggested based on the presence of spectral features, these fits cannot be confirmed. The imaging detector employed here has demonstrated significant utility in the analysis of coatings. In addition to spectroscopically discerning the differences between the top and bottom surfaces of the coating, it is easy to resolve and evaluate the degree of heterogeneity in the coating, with regards not only to surface-segregating functionality, but also to apparent polymer density and porosity. The ability to discern local polymer orientation information across a coating would be of potential use in further coating investigations.

Methocel was detected using confocal Raman, ATR-FTIR, and NEXAFS spectroscopy. This thickening agent added to the paint stripper appears to deposit as a conformal coating on the sample. The presence of phenol was seen to degrade the underlying polyurethane sufficiently as to result in breaches of the conformal coating, exposing the underlying paint to XPS analysis.

Contact Angle and Surface Free Energy

Contact angle for water and diiodomethane were obtained in order to determine the surface free energy of these coatings. The water contact angle measures the hydrophobicity of the coating while the surface free energy measures the total interaction of the surface including van der Waals and polar interactions [16, 17]. The contact angle of water varied for the full and partial formulations of the coatings, revealing how much the different fillers and pigments can affect the surface of a paint coating. The variations can be seen in Table 7 which highlights the changes in the water contact angle and surface free energy for the different coating systems.

Table 7: Water Contact Angle and Surface Free Energy of Coatings

Coating	Contact Angle (°)	Surface Free Energy (dynes/cm ²)
MIL-PRF-53039	98.70	28.21
Partially Formulated MIL-PRF-53039	94.40	34.76
MIL-PRF-85285	110.30	35.76
Partially Formulated MIL-PRF-85285	81.20	35.65

The water contact angles and surface free energy for both formulations of MIL-PRF-53039 are different and shows that surface free energy is related to water contact angle. The large difference in water contact angle between the MIL-PRF-85285 coatings and very small difference between the surface free energy reveals the usefulness of utilizing both values and that surface free energy allows for analysis of more than hydrophobicity. The changes in both water contact angle and surface free energy allow for an understanding of the bulk chemical and physical changes that are occurring to the coatings when exposed to the paint stripping solutions [18]. The data obtained for the contact angle and surface free energy are shown in the following figures 23 & 24.

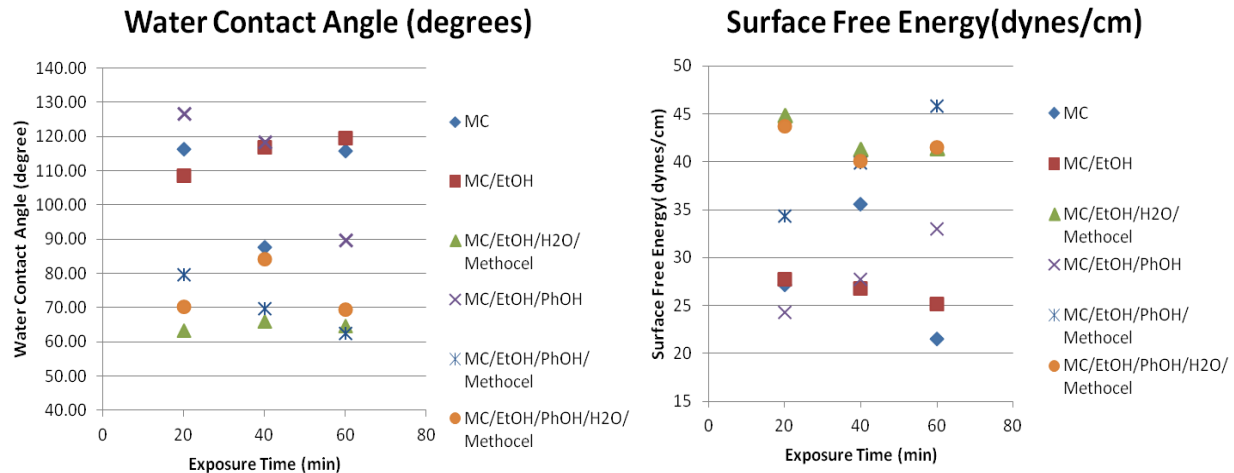


Figure 23: Contact Angle and Surface Free Energy of MIL-PRF-53039 exposed to paint stripper solutions

While the data appears sporadic, important trends and information can be determined about the method through which MIL-PRF-53039 is degraded. In both the water contact and the surface

free energy the methylene chloride, methylene chloride/ethanol and the methylene chloride/ethanol/phenol exposed samples all have similar values for the 20 minute exposure. These solutions don't contain methocel while all the paint stripper solutions that do contain methocel have similar values for the 20 minute exposure of MIL-PRF-53039. The grouping of the solutions containing methocel and the ones without generally continues through to the 60 minute exposures. This trend shows that the solutions containing methocel had approximately a 30 degree lower water contact angle and about a 14 dynes/cm² higher surface free energy. The earlier microscopic and spectroscopic evidence of methocel on the coating and these data provides further proof that methocel has deposited on the surface of the coating. Furthermore the surface energy of the coating exposed to methocel is around 45 dynes/cm² and methocel film has a surface energy of 45 dynes/cm² [19]. The main exception to the coatings following the trend of whether methocel is present is the exposure of MIL-PRF-53039 to the solution of methylene chloride/ethanol/phenol. The values for both the water contact and surface free energy start near the other solutions without methocel but then trend in the opposite direction. The increasing trend of the surface free energy for the methylene chloride/ethanol/ phenol exposure implies that the coating is undergoing a chemical change. In previous work it has been shown that phenol attacks the coating.[8] Knowing that phenol has been shown to degrade coatings and that the exposures to methylene chloride and the methylene chloride/ethanol solutions gives a different trend in the contact angle and surface free energy provides further evidence that the phenol is degrading the coating. Analysis of the MIL-PRF-85285 coatings provides similar results with a sporadic nature that contains important trends.

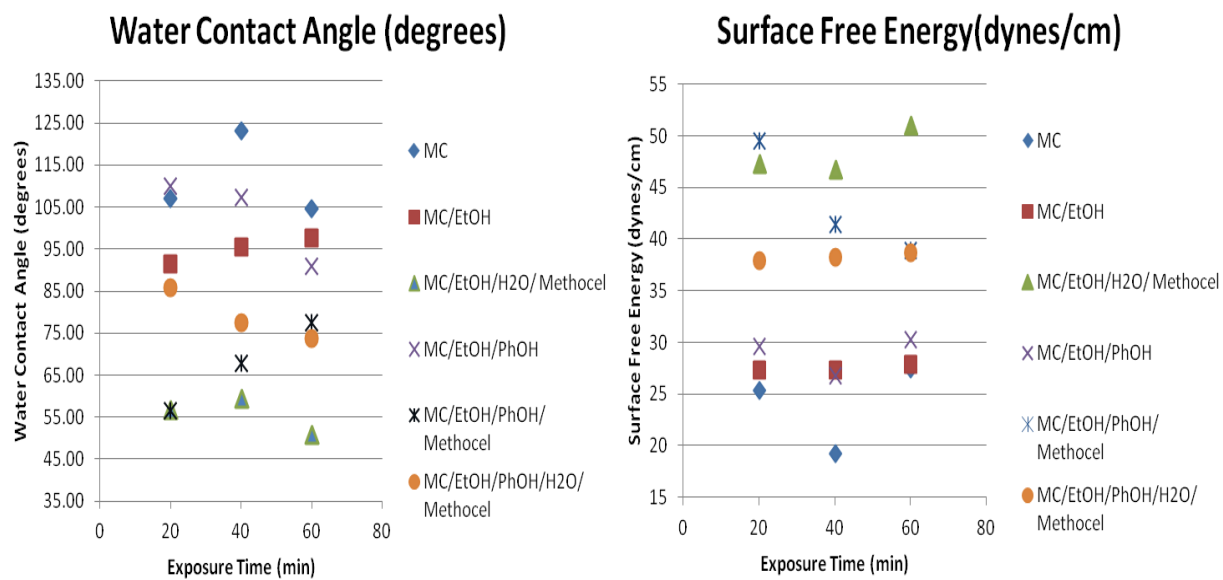


Figure 24: Contact angle and surface free energy of MIL-PRF-85285 exposed to paint stripper solutions

Comparing Figure 23 and Figure 24 many similarities exist. The initial grouping of the samples exposed to the solutions containing methocel and the ones without methocel. As with MIL-PRF-53039 not everything follows the trend once again showing the complexity of the method of attack for the paint stripper. The important differences between the two different coatings exposures are that the methylene chloride/ethanol/phenol samples trends closer to the other solutions containing methocel. The methylene chloride/ethanol/phenol/methocel exposed samples appear to start with the methylene chloride/ethanol/water/methocel samples at 20 minute exposure and then trend almost linearly to the methylene chloride/ethanol/phenol/water/methocel exposed samples at the 60 minute exposure. The smaller variance from the other samples exposed to the solutions without methocel shows that the phenol is in some way slowed in its attack on the MIL-PRF-85285 coating. The trend of the methylene chloride/ethanol/phenol/methocel sample toward the methylene chloride/ethanol/phenol/water/methocel solution, closest to the actual paint stripper, shows that while the phenol still appears to be causing degradation that the methocel may play a significant role. The method of attack for the two different coatings appears to be slightly different. Given this information phenol may need an activator or isn't the only chemical responsible for the degradation seen.

Overall all the samples from both coating systems had similar trends related to whether methocel was present in the exposure solution. Also all the exceptions contained phenol further reinforcing that phenol reacts with the coating causing degradation.

Roughness Analysis

The confocal microscope laser allows for the measurement of the height of the sample with a step of 60 nm. From the height measurements the roughness of the sample can be determined. The roughness was used in order to allow comparisons from sample to sample since it normalizes the results. The root mean square roughness was determined using the LEXT software with a cutoff of 80 μm . Utilizing the microscope at this cutoff gives the micro-scale roughness of the coatings. The roughness of the coatings surface will change as it gets degraded. The change will result from the formation of pores and cracks, removal of fillers and pigments and the chemical attack on the polymeric backbone of the coating [20, 21].

Table 8: Roughness of MIL-PRF-53039

MIL-PRF-53039 exposure	Roughness (μm)
No exposure	1.86
MC 20 min	2.12
MC 40 min	1.76
MC 60 min	2.24
MC/EtOH 20 min	2.24
MC/EtOH 40 min	2.16
MC/EtOH 60 min	2.49
MC/EtOH/H ₂ O/Methocel 20 min	1.74
MC/EtOH/H ₂ O/Methocel 40 min	1.59
MC/EtOH/H ₂ O/Methocel 60 min	1.38
MC/EtOH/PhOH 20 min	2.15
MC/EtOH/PhOH 40 min	2.01
MC/EtOH/PhOH 60 min	1.55
MC/EtOH/PhOH/Methocel 20 min	1.93
MC/EtOH/PhOH/Methocel 40 min	1.35
MC/EtOH/PhOH/Methocel 60 min	1.21
MC/EtOH/H ₂ O/PhOH/Methocel 20 min	1.85
MC/EtOH/H ₂ O/PhOH/Methocel 40 min	1.67
MC/EtOH/H ₂ O/PhOH/Methocel 60 min	1.44

The change in roughness for MIL-PRF-53039 exposed to methylene chloride and methylene chloride/ethanol was sporadic with an overall increase in roughness, as seen in Table 8.

Methylene chloride solvates the exposed coatings rearranging the fillers and pigments in the polymer network, which results in the sporadic nature of the roughness change for the samples exposed to just methylene chloride and methylene chloride/ethanol solutions. The samples exposed to all the other paint stripper solutions had a decreasing trend. The other paint stripper solutions that have a decreasing trend also contain methocel, with one exception, which was shown earlier to deposit on the surface of the coating. The deposition of the methocel film on the coating could fill in the cracks and crevices of the coating giving a lower roughness.

Comparing the data from the methylene chloride/ethanol/phenol and methylene chloride/ethanol/phenol/methocel exposures it can be seen that the solution with methocel has lower roughness at every interval. This gives good evidence that the methocel film is decreasing the roughness by depositing on the coating. It's important to remember that the methocel deposition was heterogeneous and incomplete when viewed through SEM and confocal therefore, not all of the reduction in roughness can be attributed to the methocel. The exception mentioned earlier is the methylene chloride/ethanol/phenol solution. This solution's decreasing roughness trend can only be attributed to phenol degrading the coating. The addition of phenol

to the methylene chloride/ethanol solution resulting in a decreasing trend provides further evidence that phenol plays a major role in degradation of the coating. The data demonstrate that when MIL-PRF-53039 is exposed to both phenol and methocel a decrease in the roughness of the coating occurs.

The roughness results for MIL-PRF-85285 are presented in Table 9. Varied slightly from the MIL-PRF-53039 result, which is expected since they are different coating systems and the previous results were slightly different.

Table 9: Roughness of MIL-PRF-85285

MIL-PRF-85285 exposure	Roughness (μm)
No exposure	2.11
MC 20 min	1.98
MC 40 min	2.65
MC 60 min	1.98
MC/EtOH 20 min	2.59
MC/EtOH 40 min	2.60
MC/EtOH 60 min	2.17
MC/EtOH/H ₂ O/Methocel 20 min	2.70
MC/EtOH/H ₂ O/Methocel 40 min	1.99
MC/EtOH/H ₂ O/Methocel 60 min	1.82
MC/EtOH/PhOH 20 min	1.93
MC/EtOH/PhOH 40 min	1.91
MC/EtOH/PhOH 60 min	1.55
MC/EtOH/PhOH/Methocel 20 min	1.86
MC/EtOH/PhOH/Methocel 40 min	2.40
MC/EtOH/PhOH/Methocel 60 min	2.31
MC/EtOH/H ₂ O/PhOH/Methocel 20 min	2.306
MC/EtOH/H ₂ O/PhOH/Methocel 40 min	2.257
MC/EtOH/H ₂ O/PhOH/Methocel 60 min	2.094

The samples exposed to methylene chloride and methylene chloride/ethanol are sporadic like in MIL-PRF-53039 due to the rearrangement of the coating. Samples exposed to the solutions containing methocel do not all have a decreasing trend unlike in MIL-PRF-53039. The data from the paint stripper solution of methylene chloride/ethanol/phenol/methocel has a sporadic but overall increase in surface roughness of the coatings. The random nature of the data could be attributed to the methocel deposition which was more sporadic on MIL-PRF-8528 than on MIL-PRF-53039 as can be seen in Figure 3. Also the other solution with methocel and phenol, methylene chloride/ethanol/water/phenol/methocel, while having a decreasing trend has high

roughness values. The initial roughness for samples exposed to the methylene chloride/water/methocel solution was also higher than the initial roughness giving further support for these observations. Despite this difference between the two coating systems the overall trend of both phenol and methocel sample exposures having a decreasing trend over time is present. The data from both the coating systems imply that the decreasing roughness seen stems from degradation and methocel deposition.

Thermal Analysis

Thermal analysis was conducted to help determine if physical and chemical changes develop upon exposure to the paint stripper solutions. DSC was used to determine the glass transition temperature (T_g). The change in the T_g and the TGA curve can be analyzed to determine the amount of degradation caused by the different paint stripper solutions [22]. TGA of the clear, partial and fully formulated coatings were examined. TGA overlay of clear MIL-PRF-53039 exposures to the different paint stripper solutions can be seen in Figure 25.

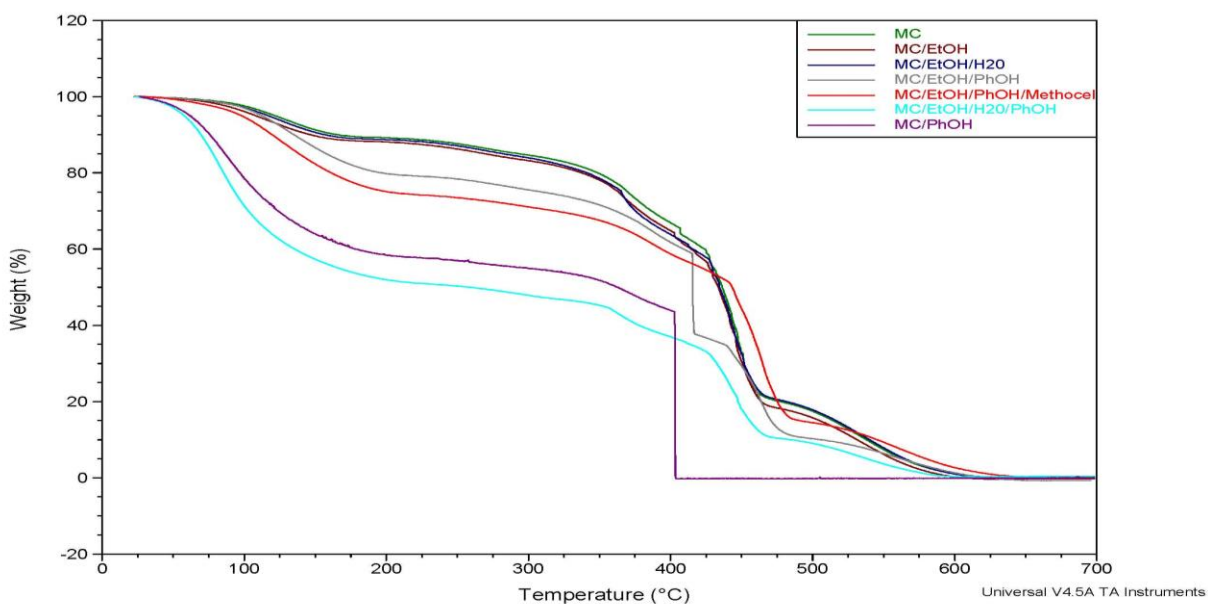


Figure 25: TGA overlay of clear MIL-PRF-53039 exposed to paint stripper solutions

The TGA of the coatings exposed to the solutions without phenol are all similar to that of methylene chloride alone. The TGA of the coatings exposed to the solutions with phenol all have significantly more weight loss. The large drop in both the methylene chloride/phenol and the methylene chloride/ethanol/phenol at 400 °C further highlights the fact that phenol degrades the coating. This drop isn't seen in the TGA of the methylene chloride/ethanol/phenol/methocel indicating that the methocel plays a role in method of attack on the coating. The TGA overlay

for the partially formulated MIL-PRF-53039, has pigments but no fillers or flatteners, exposures can be seen in Figure 26.

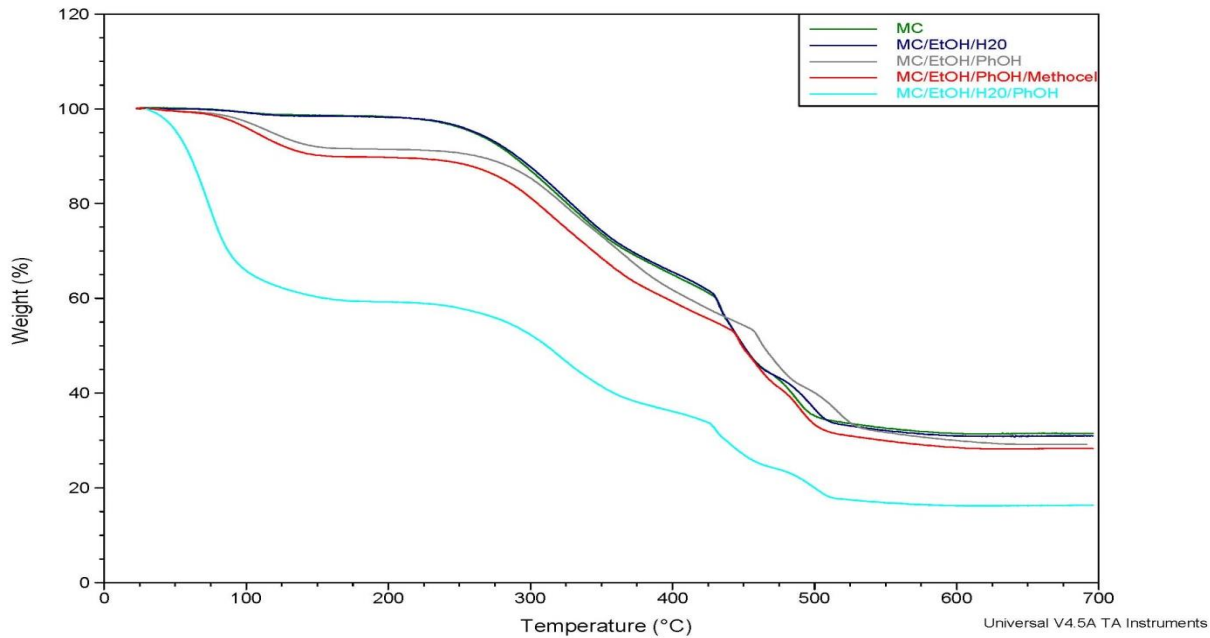


Figure 26: TGA overlay of partially formulated MIL-PRF-53039 exposed to paint stripper solutions

The TGAs for the partially formulated MIL-PRF-53039 are similar to the clear MIL-PRF-53039 with the solutions containing phenol causing the larger degradation. The sample exposed to the methylene chloride/ethanol/water/phenol/methocel solution causing larger degradation of the coating at all points than the other two solutions containing phenol. The only difference between the methylene chloride/ethanol/water/phenol/methocel solution and the methylene chloride/ethanol/phenol/methocel is the addition of water. The large increase in degradation therefore must be an effect of the water on the chemistry of the paint stripper. This implies that the water has a synergistic affect with the phenol to degrade the coating. The fact that the methylene chloride/ethanol/water solution tracks the methylene chloride solution shows that water doesn't cause significant degradation by itself and most likely acts as an activator for the phenol. The weight percent didn't reach zero for this coating due to the inorganic pigments which remain on the pan. The TGA overlay for MIL-PRF-53039 exposures is shown in Figure 27.

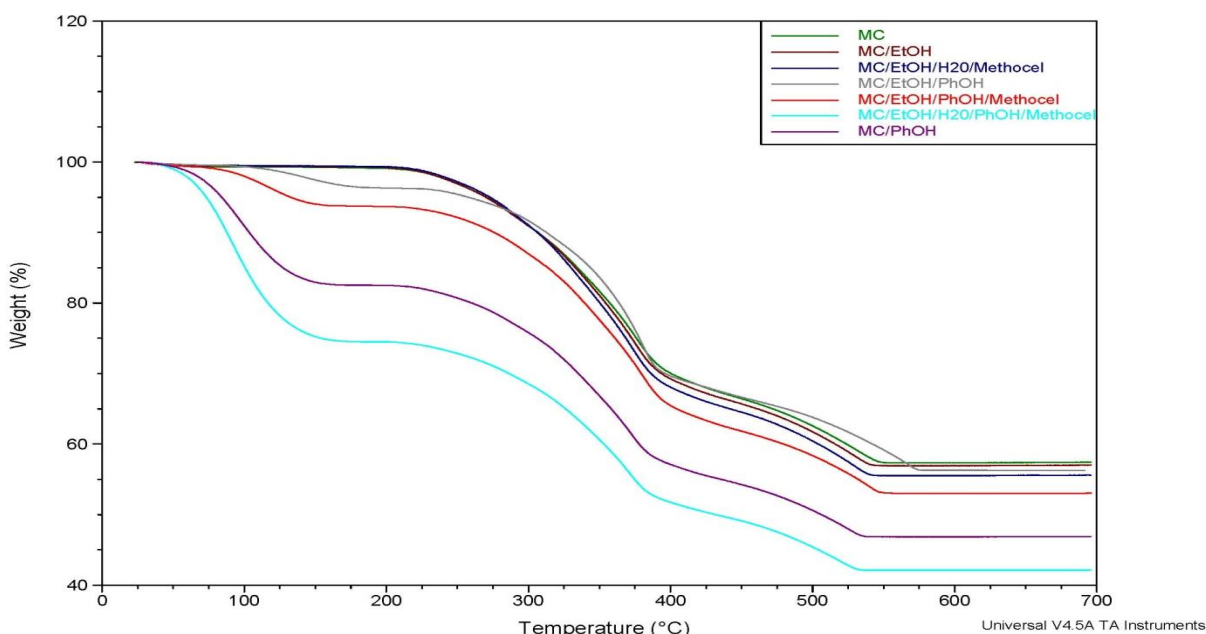


Figure 27: TGA overlay of MIL-PRF-53039 exposed to paint stripper solutions.

The TGAs for MIL-PRF-53039 are similar to both the clear and the partial formulation with the phenol solutions causing degradation and the synergistic effect the water plays with phenol. The synergistic effect can be seen even more by comparing the methylene chloride/phenol and the methylene chloride/ethanol/water/phenol/methocel exposures. The methylene chloride/phenol solution should cause significant degradation since methylene chloride solvates the coating and the phenol attacks the coating. Despite this the methylene chloride/ethanol/water/phenol/methocel exposure shows the largest degradation once again implying a synergistic effect between the components of the solution. The large degradation seen in the most complete solution of paint stripper reveals that a combinatorial effect is necessary for efficient paint stripping. The TGA overlay of clear MIL-PRF-85285 exposures can be seen in Figure 28.

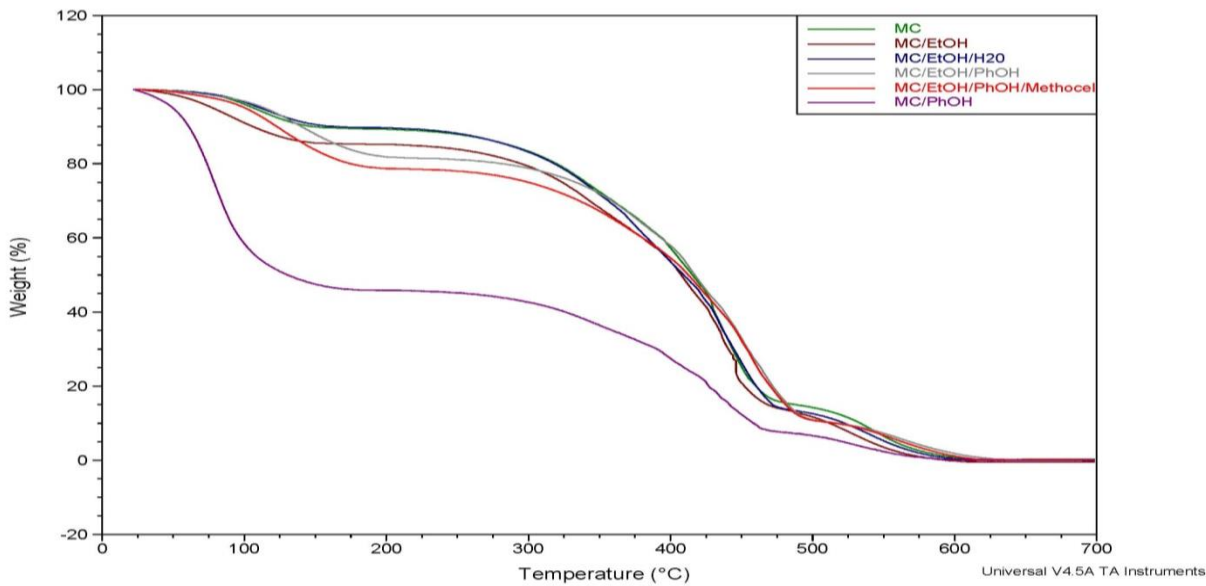


Figure 28: TGA overlay of clear MIL-PRF-85285 exposed to paint stripper solutions.

As with MIL-PRF-53039 the solutions without phenol have very similar TGAs to methylene chloride alone. Also the same as in MIL-PRF-53039 the solutions containing phenol caused significant degradation of the coating and the methocel appears to have slightly increased the degradation. Clear MIL-PRF-85285 decomposed into small pieces upon exposure to the methylene chloride/ethanol/water/phenol/methocel solution and TGA analysis was not possible. The TGA overlay of the partially formulated MIL-PRF-85285 exposures can be seen in Figure 29.

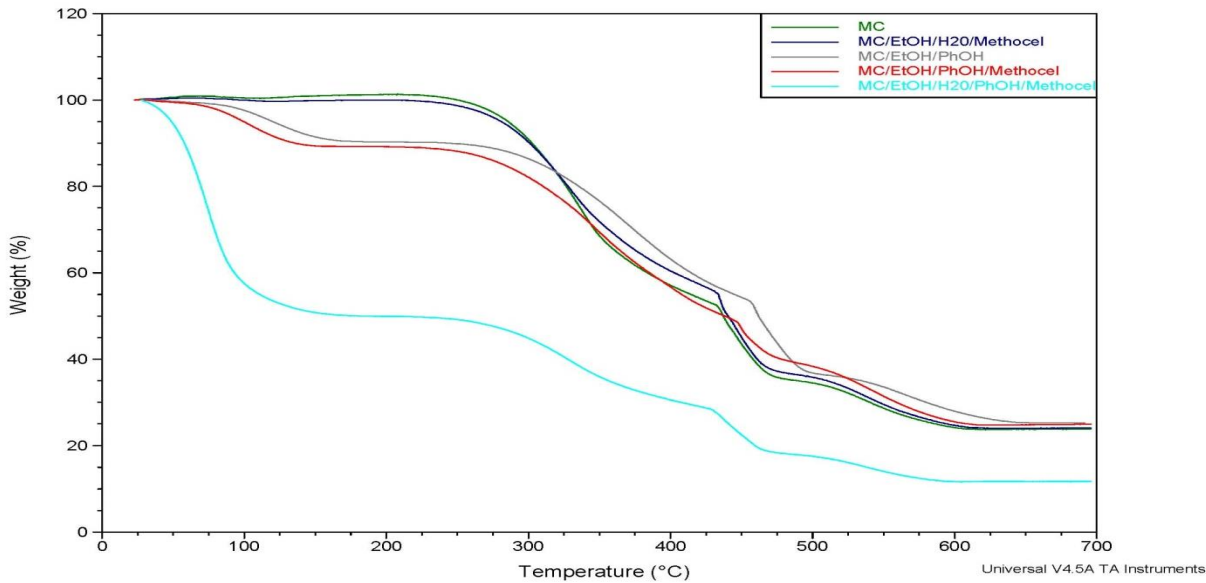


Figure 29: TGA overlay of partially formulated MIL-PRF-85285 exposed to paint stripper solutions

All the trends and observations seen in the clear coating exposures are evident in the partial formulation of MIL-PRF-85385. The synergistic effect of water and phenol seen in the methylene chloride/ ethanol/water/phenol/methocel solution is even more apparent here than in the TGAs of MIL-PRF-53039. The TGA overlay of MIL-PRF-85285 exposures can be seen in Figure 30.

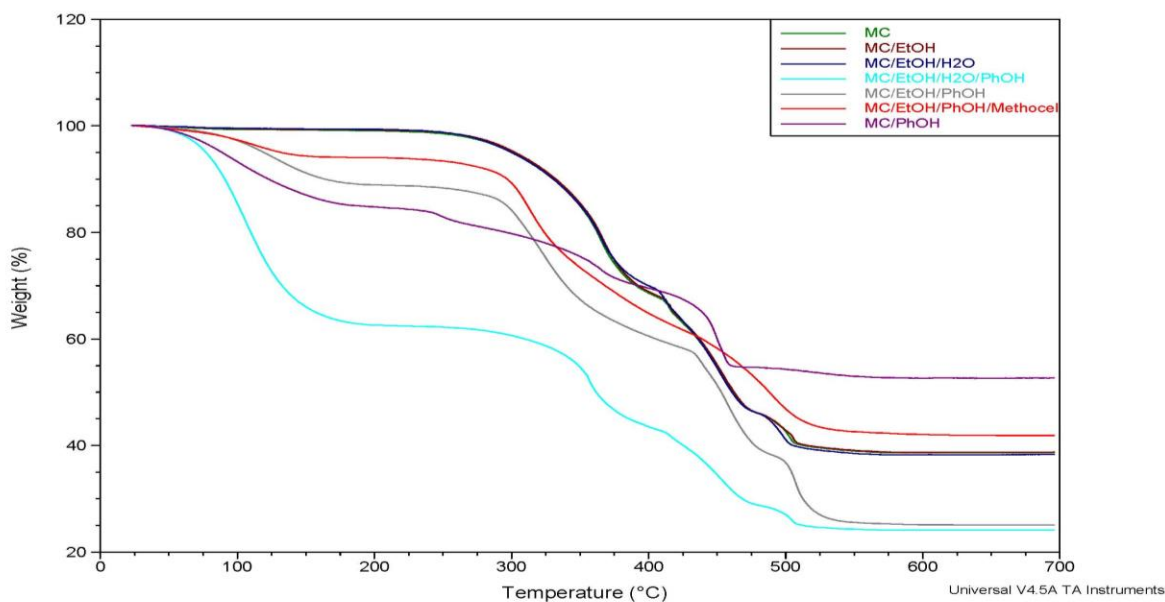


Figure 30: TGA overlay of MIL-PRF-85285 exposed to paint stripper solutions

The TGAs for samples exposed to solutions without phenol look very similar to the clear and partial formulations. The TGAs for samples exposed to solutions with phenol have a few differences. The methylene chloride/phenol solution caused significant degradation initially then plateaus before all other solution at about 480 °C. This was unexpected since in all the MIL-PRF-53039 and clear MIL-PRF-85285 coatings the methylene chloride/phenol solution caused significant degradation throughout the entire TGA run. The other odd trend is that the methylene chloride/ethanol/phenol/methocel solution exposure caused less degradation than did the methylene chloride/ethanol/phenol solution. This result is the opposite of the other MIL-PRF-85285 and MIL-PRF-53039 coatings. Both of these differences are a product of the fillers and flatteners being added to the coating. The fillers and flatteners change the coating significantly, enough to alter the method of attack for the paint stripper, highlighting how important it is to examine all the aspects of the coating system.

The TGA results for both MIL-PRF-53039 and MIL-PRF-85285 showed that the paint stripper solution with phenol cause more degradation than those without. That water and phenol have a synergistic effect increasing the degradation and that the filler and flatteners present in the coating can alter the method of attack and amount of degradation seen in the coating.

The glass transition temperatures, T_g , determined by DSC for the exposed coating is listed in Table 10.

Table 10: Glass Transition Temperatures of exposed coatings

Glass Transition Temperatures (T_g) in °C						
Solvent Exposure	AFTC MIL-PRF-85285			CARC MIL-PRF-53039		
	Clear Formulation	Partial Formulation	Full Formulation	Clear Formulation	Partial Formulation	Full Formulation
Control (no exposure)	51	65	0	87	64	60
Methylene Chloride	46	65	15	67	67	76
Methylene Chloride/Ethanol/Water/Methocel	45	65	26	70	66	81
Methylene Chloride/Ethanol/Phenol	22	31	29	44	40	53
Methylene Chloride/Ethanol/Phenol/Methocel	16	53	25	33	32	36
Methylene Chloride/Ethanol/Water/Phenol/Methocel	DECOMP	-19	-38	-11	-25	-8

For all of the coatings the exposure to methylene chloride changed the T_g very little. This is also true for the methylene chloride/ethanol/water/methocel solution with the exception of the full formulation of MIL-PRF-85285. In the clear and partial formulations of both coatings a sizable decrease in the T_g was observed upon exposure to the methylene chloride/ethanol/phenol. The presence of phenol in the solution caused degradation in the coatings as was previously observed. While this is not as apparent in the fully formulated coating indicating that the fillers and flatteners may hinder the reaction of phenol with the polymer backbone of the coatings. The methylene chloride/ethanol/phenol/methocel exposed coatings have different T_g 's than the methylene chloride/ethanol/phenol exposed coatings; giving further proof that methocel plays a role in the paint stripping process. The largest change in T_g for all the different coatings was seen from the methylene chloride/ethanol/water/phenol/methocel solution. The clear MIL-PRF-

85285 completely decomposed and the smallest change in T_g was 38 °C. Clearly this solution degrades the coating significantly. These T_g results are further evidence that the water and phenol have a synergistic effect on degradation of coatings.

The MIL-PRF-85285 results differ from all the MIL-PRF-53039 coatings and even from the clear and partial MIL-PRF-85285, similar to the TGA curves. For MIL-PRF-85285 the methylene chloride/ethanol/water/methocel, methylene chloride/ethanol/phenol and methylene chloride/ethanol/phenol/methocel solutions all have similar T_g s. The slight changes indicate which paint stripper formulation is causing more degradation on the coating however the three formulations are only separated by 4 °C. Indicating that they all affected the coating's T_g to a similar degree. The only significant change in T_g for MIL-PRF-85285 comes from the methylene chloride/ethanol/water/phenol/methocel solution. The T_g and TGA data for MIL-PRF-85285 indicate that the synergistic effect of water and phenol is essential for removal of this coating in paint stripping. The reason that the synergistic effect of water and phenol is more apparent in MIL-PRF-85285 than MIL-PRF-53039 is due to the different polymer backbone and the different fillers and flatteners in the coatings. The T_g data match the TGA curves and both reinforce the observations seen from the other techniques used to analyze the coatings.

Solution Ingress/Egress

Methocel's effect on the paint stripper solutions degradation of the coatings can be seen throughout the paper. In order to better understand the effect of the methocel deposition on the coating degradation a simple wetting analysis was done using contact angle. The purpose of this was to see if a quantitative or qualitative result could be obtained to indicate how methocel affects the paint stripper. The dynamic contact angle of methylene chloride/ethanol/phenol paint stripper solution was found on both partial and full formulation MIL-PRF-85285 and MIL-PRF-53039. Then the time it took for the paint stripper to totally wet the surface was determined. The methylene chloride and methylene chloride/ethanol solutions were unusable because they evaporated too quickly. Figure 31 shows a drop of methylene chloride/ethanol/phenol wetting the surface over a 10 second span.

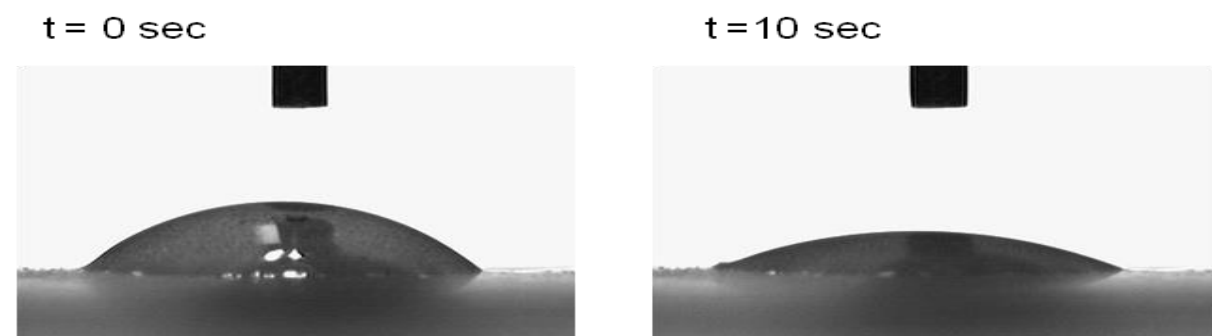


Figure 31: Methylene Chloride/Ethanol/Phenol wetting MIL-PRF-85285

The dynamic contact angle values and wetting times were obtained for the unexposed coatings, Table 11, utilizing the camera on the contact angle. The videos were taken at 17 frames per second.

Table 11: Dynamic contact angle and complete wetting time of unexposed coatings

Unexposed Coating	Dynamic Contact Angle	Time for Complete Wetting
MIL-53039	31.90°	30 sec
MIL-53039 partial formulation	N/A	≈5 sec
MIL-85285	21.00°	18 sec
MIL-85285 partial formulation	16.70°	10 sec

The unexposed coatings all showed very short wetting times with the longest, MIL-PRF-53039, being only 30 seconds. The short wetting time is expected since the paint stripper's designed to penetrate and degrade the coating. The very low contact angles also fit the quick time for complete wetting. The contact angle on MIL-PRF-53039 partial formulation was very low to begin with and then decreased quickly which resulted in the value of essentially zero or N/A. In order analyze the possible effects of methocel deposition the contact angle and wetting time of coatings exposed to methylene chloride/ethanol/water/phenol/methocel were determined.

Table 12: Dynamic contact angle and complete wetting time of exposed coatings

MC/EtOH/H₂O/PhOH/Methocel Exposed Coatings	Dynamic Contact Angle	Time for Complete Wetting
MIL-53039	34.10°	90 sec
MIL-53039 partial formulation	38.60°	125 sec
MIL-85285	41.00°	40 sec
MIL-85285 partial formulation	40.70°	100 sec

The contact angle increase slightly for all the coatings however all showed a large increase in the total wetting time. The large increase in wetting time means that the paint stripper doesn't penetrate the coating quickly. The film of methocel and the degradation on the surface of the coating are slowing the ingress of the paint stripper solution. The inhibited ingress can be viewed in the opposite direction. This means that once the paint stripper solution is in the coating the methocel film and surface degradation inhibit the solution's egress. Methocel's ability to increase the retention of the paint stripper solution in the coating reveals why the confocal

microscope, TGA and DSC data showed that the methylene chloride/ethanol/phenol/methocel solutions degradation was greater than the methylene chloride/ethanol/phenol solution. Methocel's role in solvent ingress/egress was unexpected considering that commercial paint strippers use it solely as an emulsifying agent and other components like paraffin wax are added to reduce the solvent egress.

Conclusion

Two component polyurethane MIL-PRF-85285 and single component polyurethane MIL-PRF-53039 topcoats were made into three formulations a clear coat, partial formulation and a full formulation. These coatings were exposed to the different control paint stripper solutions and then examined using confocal microscopy, SEM, XPS, FTIR-ATR, Raman, NEXAFS, TGA, DSC, and contact angle. The analysis of the microscopy showed that the solutions containing phenol caused significant degradation and that sporadic film deposition was occurring on the surface of coatings exposed to solutions containing methocel. To help analyze methocel's role in the degradation of the coatings two new solutions were made, methylene chloride/ethanol/phenol and methylene chloride/ethanol/phenol/methocel. Spectroscopic techniques were utilized to examine the degradation and confirm the presence of methocel. FTIR-ATR and Raman allowed for identification of methocel on the surface of the coatings exposed to solutions containing methocel. XPS confirmed methocel on the surface of the coatings and showed that degradation is occurring in the paint stripper solutions with phenol. NEXAFS analysis further confirmed that methylene chloride solvates and reorders the coating and that phenol degrades the coating systems. Contact angle of water and surface free energy of the coatings was determined before and after exposure. The contact angles varied for the different formulations of MIL-PRF-85285 and MIL-PRF-53039, indicating the effect that different polymer backbones, pigments and flatteners have on the coating system. While the data were sporadic the surface free energy and water contact angle of the coatings exposed to the solutions with phenol and the solutions without phenol grouped together, another indicator that phenol is the main agent of degradation. The surface free energy for the coating containing methocel was similar in value to the surface free energy of methocel, further proving that the film on the surface of the coating is methocel. Roughness analysis was conducted using the confocal microscope. The paint stripper solutions of methylene chloride and methylene chloride/ethanol caused small sporadic changes with no clear trend for both MIL-PRF-53039 and MIL-PRF-85285. The coatings exposed to methocel and/or phenol all decreased in surface roughness. This indicates that methocel deposition smoothes out the coating by filling in the valleys on the surface and that the degradation of the coating also results in a smoothing effect on the surface. The TGA curves and Tg data of the exposed coating further confirms that phenol degrades the coating. Comparing the methylene chloride/ethanol/phenol and methylene chloride/ethanol/phenol/methocel exposed coatings shows that the addition of methocel slightly increased the degradation. Comparison of the methylene chloride/ethanol/phenol/methocel and the methylene chloride/ethanol/water/phenol/methocel exposed coatings indicates that water acts synergistically with phenol to

degrade the coatings. The wetting behavior of the paint stripper solutions was examined on unexposed coating and coatings exposed to solutions containing methocel. The results showed that the methocel deposited on the surface of the coating slowed the wetting or ingress of the solution into the coating. This implies that the deposited methocel slows the egress of the paint stripper solution from the coating thereby increase the degradation. The data from this and previous work have shown that methylene chloride solvates the coating and phenol is the main agent of degradation. The work presented showed water's importance in degradation and how methocel not only emulsifies the solution but increased the degradation by depositing on the surface and trapping the solution inside.

Acknowledgements

We would like to thank SERDP for their support of this project and previous work. We also recognize the work done by Jack Kelley, James Yesinowski, Kelly Watson, Nick Nesteruk and Tom Braswell on the previous report which this work continued to research. Jack Kelley, Nick Nesteruk and Tom Braswell of Army Research Lab at Aberdeen Proving Ground on the development and formulation of the clear and partially formulated coatings used in this work. James Yesinowski of the Naval Research Lab on the NMR work done and Kelly Watson on the GCMS and initial thermal analysis work. This report would not be possible without the hard work already accomplished by them that can be found in the previous report, reference 8.

Literature Cited

Meetings

Watson, K.E.; Wynne, J.H. Yesinowski, J.P.; Young, C.N.; Clayton, C.R. "Role of Methylene Chloride and Phenol in Chemical Paint Strippers" 41st Annual ACS Mid-Atlantic Regional Meeting, April 11, 2010; paper 212.

Watson, K.E.; Wynne, J.H.; Lundin, J.G.; Yesinowski, J.P. "Novel Environmentally Friendly Approach to Paint Strippers Based in Interfacial Mechanistic Studies" 240th Annual ACS National Meeting, August 25, 2010; Boston, MA, poster 281.

Watson, K.E.; Wynne, J.H.; Yesinowski, J.P. "Progress Toward Understanding the Mechanism of Action in Methylene Chloride/Phenol Based Paint Strippers" 2010 Partners in Environmental Technology Technical Symposium & Workshop, December 1, 2010, Washington, DC, poster 50, abstract #42.

Young, C. N.; Clayton, C.R. "Spectroscopic analysis of the effects of methylene chloride- and phenol-based paint stripping solvent exposure on model coating systems" 2010 Partners in Environmental Technology Technical Symposium & Workshop, December 1, 2010, Washington, DC, poster 69, abstract #313

Wynne, J.H.; Watson, K.E.; Yesinowski, J.P.; Young, C.N.; Clayton, C.R.; Nesteruk, N.; Kelley, J.; Braswell, T. "Interim Report on Scientific Basis for Paint Stripping; Mechanism of Methylene Chloride Based Paint Removers" NRL Memorandum Report # NRL/MR/6120-10-9303.

Watson, K.E.; Wynne, J.H. Yesinowski, J.P.; Han, Y.; Young, C.N.; Clayton, C.R. "Mode of action of chemical paint strippers in removing robust polymeric coatings" 242nd ACS National Meeting and Exposition, August 31, 2011, Denver, CO, poster 14553.

Watson, K.E.; Wynne, J.H.; Yesinowski, J.P.; Han, Y.; Young, C.N.; Clayton, C.R. "Chemical paint strippers: understanding how methylene chloride and phenol remove polymeric coatings" 42nd Annual ACS Mid-Atlantic Regional Meeting, May 2011, College Park, MD.

References

- [1] J. Durkee, *Metal Finishing*, 2009, **107**, 49.
- [2] T. Wollbrinck, *Journal of the American Institute for Conservation*, 1993, **32**, 43.
- [3] S. Spring, *Metal Finishing*, 1959, **57**, 63.
- [4] V. Del Nero, C. Siat, M. J. Marti, J. M. Aubry, J. P. Lallier, N. Dupuy and J. P. Huvenne, in *The proceedings of the 53rd international meeting of physical chemistry: Organic coatings*, AIP, Paris, France, 1996, pp. 469.
- [5] K. R. Stone and J. Springer Jnr, *Environmental Progress*, 1995, **14**, 261.
- [6] S. G. Croll, *Journal of Coatings Technology Research*, 2009, **7**, 49.
- [7] V. P. Volkov, K. V. Nel'son, E. N. Sotnikova, N. P. Apukhtina and L. I. Potepun, *Journal of Applied Spectroscopy*, 1982, **36**, 557.
- [8] Wynne, J. H., Watson, K. E., Yesinowski, J. P., Young, C. N., Clayton, C. R., Nesteruk, N., Kelley, J., Braswell, T., *NRL/MR/6120--11-9368* 2011 Naval Research Laboratory.
- [9] Wollenweber, C., A. V. Makievska, et al., *Colloids and Surfaces a-Physicochemical and Engineering Aspects*, 2000, **172**, 91.
- [10] Patterson, B. M. and G. J. Havrilla., *Applied Spectroscopy*, 2006, **60**, 1256
- [11] Urquhart SG, Hitchcock AP, Smith AP, Ade HW, Lidy W, Rightor EG, et al., *Journal of Electron Spectroscopy and Related Phenomena*, 1999, **100**, 119.
- [12] Urquhart SG, Smith AP, Ade HW, Hitchcock AP, Rightor EG, Lidy W., *The Journal of Physical Chemistry B*, 1999, **103**, 4603.
- [13] Kuznetsova A, Popova I, Yates JT, Bronikowski MJ, Huffman CB, Liu J, et al., *Journal of the American Chemical Society*. 2001, **123**, 10699.
- [14] Sedlmair J., Soft X-Ray Spectromicroscopy of Environmental and Biological Samples. Universitätsverlag Göttingen, 2011.
- [15] Lenhart JL, Fischer DA, Chantawansri TL, Andzelm JW., *Langmuir*. 2012, **28**, 15713.
- [16] Owens, D. K., and Wendt, R. C., *Journal Applied Polymer Science* 1969, **13**, 1741
- [17] Jurak, M., and Chibowski, E., *Langmuir*, 2006, **22**, 7226
- [18] Ploeger, R., S. Musso, et al., *Progress in Organic Coatings*, 2009, **65**, 77.
- [19] Khan, H., J. T. Fell, et al., *International Journal of Pharmaceutics* 2001, **227**, 113.
- [20] Rashvand, M., Z. Ranjbar, et al., *Progress in Organic Coatings*, 2011, **71**, 362.

- [21] Mirabedini, S. M., M. Sabzi, et al., *Applied Surface Science*, 2011, **257**, 4196.
- [22] Newkirk, A. E., *Analytical Chemistry* 1960, **32**, 1558.
- [23] Janigova, I., I. Lacik, et al., *Polymer Degradation and Stability*, 2002, **77**, 35.